PREDICTION OF BIOFILM THICKNESS IN HOLLOW FIBER BIOREACTORS

By

CHUN LI

Bachelor of Science

Sichuan Union University

Sichuan, China

1997

Submitted to the Faculty of the
Graduate College of the
Oklahoma State University
in partial fulfillment of
the requirement for
the Degree of
MASTER OF SCIENCE
July, 2000

PREDICTION OF BIOFILM THICKNESS IN

HOLLOW FIBER BIOREACTORS

Thesis Approved:

Randy S. Lewis

Thesis Adviser

Laura Hugh

Alva H. Johannes

Alfred Larson

Dean of the Graduate College

ACKNOWLEDGEMENTS

I would like to express my sincere appreciation to my advisor, Dr. Randy Lewis for his guidance, supervision, and help throughout all the process of research. I would also like to thank my other committee members Dr. Johanna and Dr. Karen High. I wish to thank Dr. Robert Miller and Grant Severson in Department of Microbiology for providing bacteria and facilities. My sincere appreciation extends to Ms. Phoebe Doss for her help on preparing samples and taking pictures.

Moreover, I would like to thank to members in our group who provided suggestions and assistance for this study: Dr. Arland Rammamurthi, Mr. Xunbao Duan.

I would also express my appreciation to Weibo, for his encouragement, love and understanding at times of difficulty. I wish to express my gratitude to my parents for their support and encouragement.

Finally, I would like to express my appreciation the Department of Chemical Engineering for supporting during these two years of study.

Table of Contents

List of Table

Table Page

List of Figures

List of Nomenclature

HFM: Hollow Fiber Membrane bioreactor

SEM: Scanning Electron Microscope

ΔP: Pressure drop, mmHg

ΔP_i: Pressure drop without cells, mmHg

ΔP_b: Pressure drop with cells, mmHg

ID: Inner diameter, mm

NT: Number of tubes

R_i: Radius of tube without cells, mm

R_b: Radius of tube with cells, mm

R: Radius of tubes, mm

L: Length of fiber units, cm

Q: Flow rate, ml/min

μ: Viscosity, g/cm s

t: Thickness of biofilm, μm

ν: Kinematic viscosity, mm^2/s

CHAPTER 1

INTRODUCTION

When cells are adjacent to a surface, they have a tendency to attach and grow on the surface, and form a biofilm. Biofilms are composed of individual cells surrounded by cellular products. Biofilms can be problematic, such as causing infections while using medical device, contaminating food, and corroding heat exchangers. However, biofilms can be beneficially used to treat waste water and waste gas to produce liquid fuel.

The biofilm thickness is one of the most important parameters for studying biofilms. Optimal biofilm thickness is essential for biofilm activity, design and optimization of bioreactors. However, most methods for studying biofilm growth and thickness disturb the system and require cessation of experiments. Therefore, realization of continuous biofilm growth and biofilm thickness observation is desirable. In this thesis, an *in-situ* method for continuous prediction of the biofilm thickness is addressed for hollow fiber reactors.

1.1 Bioreactor types

Bioreactors are devices used to biochemically transform materials by living cells or cell-free enzymes system. These reactors have been widely used in fermentation processes, in waste treatment, and in antibody production (Blanch et al., 1997).

There are three general bioreactor systems in which cells are utilized: freely suspended cells, cell attached to surfaces as biofilms and encapsulated cells. Several types of bioreactors incorporate the above methods, including stirred tank reactors, rotary

drum tank reactors, bubble columns, and plug flow reactors. Stirred tank bioreactor with bubble aeration developed by impellers provides control and flexibility in mixing and aeration. Thus, stirred tanks are the most frequently used bioreactors. However, high shear stresses leading to cell death and high power consumption are the main limitations. Plug flow reactors are often applied for optimal utilization of substrates and oxygen (Sajc et al., 1999). Bubble column bioreactors are advantageous with regards to low investment requirements due to their simple construction and low energy requirements (Schugerl, 1977).

Many bioreactors can be used for suspended cell culture, such as stirred tank reactors, bubble column reactors, and activated sludge reactors. In suspended cell culture processes, the important advantages are homogeneous suspension in the reactor, high oxygen consumption rate, high biomass concentration, and stable biological operation. Among these, the suspension homogeneity and transport rate of nutrients are especially important for large-scale and high-density cultures. However, high shear stress, large volume of reactor, low treatment capacity, and sediment removal are major disadvantages of suspended cell culture (Lazarova et al., 1994, Prokop et al., 1989).

Not all cells grow in suspension, especially fragile mammalian cells. Encapsulated cell cultures provide one method to solve this problem. In this kind of reactor, cells are entrapped or compartmentalized in a defined region, such as a fiber or gel. Stirred tanks or membrane bioreactors are often used for encapsulated cell culture. The physical support helps protect fragile cells against shear stress and stabilize the cells. Encapsulated cells are an ideal method for researchers to study interactions between cells and genetically monitor cell growth. The disadvantages of encapsulation are

inaccessibility of cells and minimum surface area due to microbead shapes (Miller et al., 1989).

Comparing the methods of utilizing cells as above, biofilm reactors are advantageous when requiring more concentrated and dense cells, which provides the possibility of higher bioreactor efficiencies and higher biomass activities. However, heterogeneity of biofilm reactors is the major disadvantage of fixed cell cultures. Biofilms can be cultured in stirred tanks, membrane bioreactors, fluidized-bed reactors, airlift bioreactors, and trickling filter reactors. Sometimes, both suspended individual cells and fixed biofilms exist in the same bioreactor, which is called mix culture (Lazarova et al., 1994).

1.2 Biofilm reactors

1.2.1 Biofilm characteristics and applications

A biofilm is composed of cellular products, such as polysaccharides in which individual cells are embedded. When plant cells, animal cells, or bacteria are adjacent to surfaces, these cells start to attach and then grow on the surface to form a biofilm (Costerton et al., 1999). After the initial attachment, biofilms continue to grow if favorable environmental conditions persist. Environmental conditions include mass transfer rates of substrate and products, culture temperature, pH, and conversion rate of the substrate by the biofilm (van Loosdrecht et al., 1995). The biofilm thickness depends on cell growth and detachment rates. If the rate of cell attachment and growth exceeds

that of detachment, the biofilm thickness continues to increase until equilibrium of attachment, growth and detachment is obtained (Cunnlngham et al., 1991).

Some biofilms are detrimental. There are concerns about biofilm formation in medical devices related to infection, such as pseudomonas aeruginosa biofilms leading to cystic fibrosis pneumonia. One major problem with treating biofilm formation is the biofilm depth and diffusion distance through the biofilm. Biofilms are also a source of contamination in food processes (Ganesh et al., 1991). Due to the same reasons mentioned above, biofilms are more resistant than free-living cells to sanitizing compounds. Biofilms can also cause environmental problems such as growth in drinking water distribution systems. Not only do biofilms grow on the pipe wall, but they release substances that promote corrosion. In addition, biofilms can decrease heat transfer rates in cooling towers by increasing frictional and heat transfer resistances (Bryers et al., 1998, Drury et al., 1993). A better understanding of biofilms can help reduce detrimental biofilm effects.

On the other hand, biofilms can be beneficial. For example, the pseudomonas alcaligenes can biodegrade phenol (Kanekar et al., 1996) and the Butyribacterium methylotrophicum can convert CO to liquid fuel such as alcohol when utilized in biofilm systems (Grethlein et al., 1990). Since bacterial cells live on carbon, bacteria cells have the potential to consume waste compounds in water and gas. Biofilms have been widely utilized in wastewater treatment, such as xanthobacter autotrophicus cells utilized to uptake dichloroethane (DCE) and other haloalkines structurally related to DCE (Freitas dos Santos et al., 1995). Other examples include the use of mycobateium Py1 and xanthobacter Py2 for propene consumption (Reij et al., 1997), pseudomonas acidovorans

CA28 cells for 3-chlorbenzoate degradation, and pseudomonas acidovorans CA28 cells for aniline and chloro-aniline degradation (Peys et al., 1997).

Biofilms are also used for the bioconversion of synthesis gas into fuels and chemicals. Synthesis gas, which contains primarily CO, H_2, and CO_2, is a major source for the production of fuels and chemicals. In 1987, a new anaerobic bacterium, clostridial ljungdahlii was isolated, which can form ethanol autotrophically, which is able to grow on CO as the sole carbon source from synthesis gas (Phillips et al., 1994, Klasson et al., 1992). Several other bacteria, such as peptostreptococcus productus strain U-1, eubacteium limosum, and butyribatereium methylotrophicum can also grow on either CO or CO_2/H_2 as their carbon and energy source to produce alcohol and acetate (Grethlein et al., 1990).

Other than bacteria, mammalian cells can be cultured to form biofilms for different purposes, such as the use of hepatocytes as an alternative to the use of animals to study drug detoxification by liver (Jauregui et al., 1998). Animal cell culture experiments have been conducted for the production of immunoglobulins, a major class of proteins that can be used for therapeutic purposes (Schweikart et al., 1999).

Biological processes have several advantages over catalytic processes, although they are generally slower than chemical reactions. The advantages of such processes are higher specificity, higher yields, and lower energy costs. Moreover, the irreversibility of many biological reactions allows complete conversion without facing thermodynamic equilibrium constraints associated with non-biological systems (Klasson et al., 1992).

1.2.2 Biofilm reactor types and usage

Several biofilm reactors have been used for cell culture. Such bioreactors include packed-bed reactors, trickling filters, biofilters, fluidized-bed reactors, rotating biological contactors, airlift reactors, turbulent reactors and membrane bioreactors. The first three reactors are classified as fix-bed reactors and the latter five are mobile-bed reactors (Pujol et al., 1994).

Fixed-bed bioreactors can be operated as filters in addition to the biological reactor function. The main disadvantage is that frequent backwash is required because of rapid clogging of the bed. In packed-bed reactors, biofilms grow on submerged inert packing beads, usually glass or polycarbonate beads. The flowing liquid phase provides microorganisms with substrates and nutrients. Trickling filters are heterogeneous bioreactors in which the biomass is fixed on inert packing and fluid trickles over the packing. They are simple to design, operate and maintain. During operation, the fluid trickles through the support material with attached cells due to gravity.

In mobile bed bioreactors, biofilm processes utilize continuously moving media by mechanical agitation, such as with rotating biological contactors, or by high air and/or water velocity such as fluidized bed reactors and turbulent reactors. The moving media operation improves mass transfer rates, reduces biofilm diffusion limitations, and accelerates biochemical reactions. Very fine or very porous granular materials are used to increase surface area for bacteria growth. In wastewater and gas treatment, due to the above advantages, mobile bed reactors provide high removal efficiencies, better oxygen transfer rates, and reduced sludge production as compared to fixed-bed reactors (Lazavoza et al., 1994).

Rotating biological contactors incorporate biofilms grown on the surface of rotating disks. The disks are partially immersed in liquid and partially into air. Low energy consumption and simple and inexpensive designs make rotating biological contactors highly favorable for wastewater treatment (Langwaldt et al., 2000). Rotating biological reactors have been applied for denitrification, nitrification of secondary and tertiary effluent, and phosphorus removal. Biofilms are reasonably uniform within each reactor compartment (Gujer et al., 1990).

There are three types of fluidized-bed bioreactors: two-phase, three-phase and inverse fluidized bed. These reactors can provide high process efficiencies and high biomass concentrations, which result in smaller reactor volumes (Hermanowicz et al., 1990). Three-phase fluidized bioreactor cultures provide more active biomass with higher mass transfer rates. With fluidized-bed bioreactors, biofilms are generally grown on granular support material (Brower et al., 1996, Langwaldt et al., 2000).

Airlift bioreactors provide excellent capacities and efficiencies because of better hydrodynamic characteristics of the reactors and high biomass concentrations. However, the sophisticated construction and scale-up are difficult to optimize and the operation is more complex (Lazarova et al., 1994).

Several studies have utilized the aforementioned reactors. Mass transfer and kinetic parameters using trickling-bed bioreactors were studied (Revah et al., 1995). Research has been done on the effects of filter medium on biofilter performance and the differences in response to varied cell mass loadings with different substrates (Corsi et al., 1996). The main parameters affecting the steady state behavior of a rotating biological contactor (RBC) have been investigated (Sassi et al., 1996). Prototheca zopfii cells were

cultured in RBC to biodegrade hydrocarbons (Yamaguchi et al., 1999). Bioconversion of 4-chlorobiphenyl and polychlorobiphenyl by an uncharacterized pseudomonas species were conducted in a fixed-bed bioreactor with glass beads (Fava et al., 1996). Biofilms were formed in a fixed-bed reactor to biodegrade pentachlorophenol (Edgehill et al., 1996). Treatment of newsprint waste water was conducted in a fluidized-bed bioreactor (Broch-Due et al., 1997). A three-phase fluidized bed reactor was applied to find out influences of hydrodynamic parameters and substrate patterns on the biofilm formation for the nitrification process (Cheng et al., 1997). The influence of reactor types and shear stress on aerobic biofilm populations were studied by comparing a batch reactor, an indoor channel reactor with recirculation and two continuous stirred tank batch reactors with different shear stresses (Cao et al., 1995).

Besides the widely used bioreactors mentioned above, Pseudomonas putida 54G was applied to a flat plate bioreactor to degrade toluene (Villaverde et al., 1997). A relatively less familiar bio-electron reactor, in which a biofilm forms on the surface of several electrodes, was used for simultaneous oxidation and reduction treatment of polluted water (Kuroda et al., 1996).

Finally, membrane bioreactors are also widely used. Membrane bioreactors are reactors utilizing organic or inorganic membranes as barriers to separate chemicals by pressure differences, concentration differences and electrical potential gradient between both sides of the membrane. Membrane bioreactors can be used for all three different forms of cell culture. High cell density, large surface area, easiness to scale up, and low shear environment are major advantages of membrane bioreactors. They are ideal for animal cell cultures. However, oxygen diffusion problems associated with membranes are

a major disadvantage. Overgrowth of cells in membrane reactors can also break the membrane.

Comparing all the bioreactors above, fluidized bed reactors, membrane bioreactors, and airlift reactors have higher efficiencies than that of others. Stirred tanks and fixed-bed reactors have lower efficiencies.

1.3 Hollow fiber membrane bioreactor

Comparing the reactors mentioned above, there are several advantages of utilizing membrane bioreactors (Drioli et al., 1999, Dijk et al., 1997):

1. Large available surface area per unit volume, which requires a smaller bioreactor size.
2. New possibilities can be explored for various immobilization surfaces, leading to enhanced enzyme stability.
3. Compartmentalization of membrane reactors provides low shear environment to protect cells from damage.
4. A higher ratio of product to culture medium derived contaminants, due to continuous removal of enzyme inhibitors.
5. Easy to scale up because of no moving parts.
6. Low labor and capital investment cost.

Widely used hydrophobic or hydrophilic membrane materials include polycarbonate, polypropylene, polyimide, PVC copolymer, cellulose acetate, and polyester. Hydrophobic membranes are usually applied for waste gas and hydrophilic

membranes for wastewater. Other membranes include inorganic materials such as glass and ceramic. These inorganic materials have a high degree of resistance to chemicals and abrasive degradation and can handle a wider range of pH and temperature (Drioli et al., 1999).

Different immobilization methods for cells for various membrane bioreactors have been applied to various biomedical, environmental and food industries. Cells can be retained on the shell side of the membrane, and nutrients are provided from the membrane lumen side. Microbial cells entrapped in capillary membrane reactors have been utilized for white wine assessments (Drioli et al., 1999).

There are several different membrane modules that incorporate the membranes. The most common membranes are flat or tubular as applied to the following configurations: Flat plate, spiral wound, shell and tube, hollow fiber and rotary disk. Among these, the hollow fiber module has a lower feed side pressure loss and concentration polarization. Concentration polarization involves an increment of the solute concentration at the membrane surface leading to a decrease in the driving force. Hollow fiber modules are composed of many capillary tubes glued together at the ends with fluid circulating within and/or without the tubes to bring oxygen (or other gases) and nutrients (Davis et al. 1992) to the cells. Compared to traditional reactors, hollow fiber bioreactors provide a much higher purity of the product and a greater available surface area per volume. Hollow fiber units have been used for waste water and waste gas treatment, production of monoclonal antibodies, proteins, viruses, and recombinant protein products (Lowrey et al., 1994). Studies have shown cells growing in hollow fiber bioreactors can reach very high densities. In addition, hollow fiber bioreactors have provided a way of

provided a way of studying complex behavior of cells in a strictly controlled environment (Drioli et al., 1999). Table 1 summarizes some work and research in various fields, especially waste treatment using hollow fiber units.

Table 1.1 Application of Hollow Fiber Module Bioreactors

Article Resources	Biofilm Compositions	Membrane Composition	Research Focus(es)
Lowrey et al., 1994	Hybridomas 3C11, African green monkey kidney cells	Cellulose, Cuprammonium Rayon, Cellulose Acetate	Bioreactor composition as an important variable in culturing cells to produce MCA (monclonal antibody).
Handa-Corrigan et al., 1992	Mouse hybridoma cells	Unknown	Optimization strategy of production of MCA (uptake rate of glucose and production rate of lactate).
Ferreira et al., 1998	Chlorella vulgaris	Microporous Polypropylene	Carbon dioxide absorption by suspended microorganisms.
Yang et al., 1998	Unknown	Stainless Steel, Silicon	Recovery of volatile gases from water.

Table 1.1 (cont.)

Article Resources	Biofilm Compositions	Membrane Composition	Research Focus(es)
Jauregui et al., 1993	Rat hepatocytes	Microporous Polysulfone	Study of drug detoxification by liver.
F. Molinari et al., 1997	Gluconobacter oxydans	Microporous polypropylene	Bioconversion of isoamyl alcohol to isovaleraldehyde.
R. Molinari et al., 1990	Proteins	Polypropylene	Ultrafiltration and affinity separation of proteins.
Nordon et al., 1997	Unknown	Unknown	Design of hollow fiber modules for affinity cell separation.
Stoll et al., 1996	Murine hybridoma	Unknown	Development of on-line control system for animal cell cultivation.
Kamo et al., 1990	Unknown	Polyurethane, polyethylene	Hollow fiber membrane as artificial lung.

Table 1.1 (cont.)

Article Resources	Biofilm Compositions	Membrane Composition	Research Focus(es)
Gramer et al., 1998	Rho 1D4 murine hybridoma cells	Silicone	Efficient screening tools for different cell lines and process conditions.
Reij et al., 1996	Xanthobacter Py2	Polypropylene	Propane removal from synthetic waste gas
Ergas et al., 1997	Unknown	Polypropylene	Toluene removal from wastewater.
Ergas et al., 1998	Pseudomonas putida To11A	Polyethylene	Comparison of toluene removal by batch reactor and hollow fiber module.
Pankhania et al., 1999	Unknown	Polypropylene	Test the ability of bioreactor to treat wastewater.

Table 1.1 (cont.)

Article Resources	Biofilm Compositions	Membrane Composition	Research Focus(es)
Parvatiyar et al., 1996	Unknown	Polysulfone	Biodegradation of toluene.
Brindle et al., 1998	Nitrosomonas sp. and Nitrobacter sp.	Polyethylene	High rates of nitrogen removal and nitrification.
Tanyolac et al., 1995	Unknown	Unknown	Mathematical model for calculation of optimum biofilm densities as a function of substrate concentration.
Capiaumont et al., 1995	Murine Hybridoma Cells	Polypropylene	Apply hollow fiber reactor to reduce ammonia in hybridoma cell cultures.
Dowd et al.,1999	Mouse hybridoma cells 341-G6	Unknown	Develop predictive control for feed rates to control glucose concentration.

CHAPTER 2

OBJECTIVE AND SPEICIFIC AIMS

To enhance the understanding of biofilm systems, many studies have been conducted with various biofilm structures, characteristics, activities, functions and mechanics. Major parameters affecting biofilm performance are the biofilm thickness, biofilm density, and limiting substrate diffusion coefficient. These parameters are essential for bioreactor optimization (Peys, et al. 1997). Among these parameters, the biofilm thickness has many important effects and will be addressed in this thesis.

2.1 Background Information

There are two definitions of biofilm thickness: total biofilm thickness and active biofilm thickness. The total biofilm thickness is the thickness from the support of biofilm to the interface between the biofilm and bulk fluid. The active biofilm thickness is the thickness where nutrients are utilized following diffusion.

Biofilm structures are highly stratified, such that they vary with biofilm depth. This is the result of competition for substrate and space, which is affected by the biofilm thickness (Bishop et al. 1995). The biofilm thickness also has an effect on the spatial distribution of biofilm properties, such as the mass transfer rate and biodegradation kinetics. For biofilm thicknesses greater than 500 μm, the spatial difference of biofilm properties, such as the increase rate of biofilm density and the decrease rate of biofilm porosity is smaller than at other thicknesses. For biofilms with thicknesses between 130-

240μm, the increase of density and the decrease of biofilm porosity are the greatest with depth. Thus, the change in density and porosity of the biofilm is larger for thin biofilms than that for thick biofilms. This is the result of a non-uniform relationship between average biofilm density and biofilm thickness. (Bishop et al., 1995).

Both the biofilm density and biofilm thickness are two essential parameters for evaluation of a biofilm reactor performance. These parameters directly affect the consumption and production rates of various species. Total reaction volume of the microorganisms and substrate consumption rate increases as the biofilm thickness increases. The biofilm density increases the reaction rate in the biofilm but it limits the diffusional transfer rate of the substrate. Hoehn and Ray (1973) discovered that the biofilm density depends on its thickness. The density changes with the biofilm depth as a result of competition between cells for space and nutrients. The biofilm density increases with increment of the biofilm thickness, then after reaching a maximum density, the biofilm density starts to decline for better substrate transfer through the biofilm (Seker et al., 1995).

Study shows that the mass transfer rates are affected by the biofilm thickness. The mass transfer coefficient increases rapidly with the biofilm thickness before the biofilm thickness reaches 100 μm. When the biofilm thickness continues to increase, the external mass transfer coefficient stays constant without a dramatic change. This may be the result of the increased surface roughness with increased biofilm thickness. The increased roughness causes the increased mass transfer. The increasing porosity and Reynolds number can also be factors for a higher mass transfer coefficient (Beyenal et al., 1998).

The increase of fluid frictional losses and heat transfer resistances can occur with the increasing biofilm thickness in industrial process equipment, and negative effects on pollutant flux and antibiotic diffusion can be caused by an increase of the biofilm thickness (Peyton et al. 1996).

Many studies have addressed the issue of the biofilm thickness for assessing and characterizing the bioreactor performance capacity. Oxygen mass transfer characteristics were studied in a membrane-aerated biofilm reactor utilizing acetate consumption. The mass transport of oxygen into the active biofilm was affected by the thickness of a biofilm that was carbon substrate starved. The oxygen limitation, acetate limitation and dual limitation for biofilm growth were studied. For equal acetate concentrations of two different biofilm thicknesess of 490 μm and 1050 μm, oxygen uptake rates differed significantly and corresponded to biofilm thickness. For thinner biofilms, a low oxygen pressure resulted in oxygen limitations. For thicker biofilms, only dual-substrate limitation was observed. At high acetate concentrations with thin biofilms, acetate was consumed completely within the biofilm; at lower acetate concentrations, oxygen limitations didn't occur because of complete penetration of oxygen into the biofilm. In thicker biofilms, neither acetate nor oxygen could penetrate completely (Casey et al., 1998).

A membrane bioreactor was applied for culturing pseudomonas putida BN210 to degrade chlorinated aromatics. The study showed that the diffusion rate of chlorinated aromatics decreased dramatically due to the presence of biomass on the membrane. The increased diffusion resistance was caused by the biofilm formation and blockage of membrane pores. An important conclusion was made that the biofilm thickness should

not increase beyond the maximum active depth to minimize the diffusion resistance, especially with regards to oxygen (Peys et al., 1997).

The performance of a biofilm in a single-tube extractive membrane bioreactor was studied. Mass balances showed that the biofilm was effective in stripping dichloroethane (DCE) from air. Experimental results showed that the biofilm has both positive and negative effects on air stripping of DCE. When the biofilm started to form the DCE mass transfer rate increased. After reaching steady state biomass attachment, the DCE mass transfer rate dropped. For this study, an optimal biofilm thickness was between 200 and 400 μm in this system (Freitas dos Santos et al., 1995).

With regards to determining the biofilm thickness, a model of a first order relationship between biofilm thickness and shear rate was developed by Rittman. Recently the effects of shear stress and substrate loading rate on pseudomonas aeruginosa biofilm thicknesses and densities were studied in an annular reactor. The result showed that the biofilm thickness increased significantly with increases in substrate loading rate but there was not a consistent relationship between thickness and increasing shear stress. Experimental results also demonstrated that biofilm roughness increased with thickness, and the roughness is approximately 20% of the measured average thickness. The biofilm roughness was defined as standard deviation from the average value of the biofilm thickness (Peyton et al., 1995).

Several mathematical models were set up to describe the detachment rate of biofilms. A first order dependence of detachment rate on biofilm thickness is one model A second order dependence of detachment rate on biofilm thickness was also proposed

by Wanner in 1986. Another model to calculate the steady state biofilm thickness was based on the net rate of synthesis of a component (Stewart et al., 1992).

Since biofilms are heterogeneous, the thickness is not usually uniform throughout the bioreactor. Average biofilm thicknesses have been used in the calculation and mathematical modeling of bioreactors. The average biofilm thickness has also been used for the estimation of net biomass accumulation.

The optimal biofilm thickness plays a key role in engineering design and operation of bioreactors (Nicollela et al., 2000). There are several ways to determine biofilm thicknesses: optical, volumetric displacement, thermal resistance and electrical conductance. For the optical method, a light microscope, scanning electron microscope (SEM), or confocal scanning laser microscope (CSLM) has been applied to directly measure the biofilm thickness. Measuring the volumetric displacement of a biofilm-covered substratum and volume of the clean substratum is another method. Determination of the thermal resistance of fixed biomass is an indirect method to determine the biofilm thickness. Measurement of the electrical conductance of biofilms on metal surfaces can be applied for the bioreactors that have metal substratum. The average biofilm thickness can be obtained by volumetric displacement, and point measurements are provided by the optical method, thermal resistance method, and electrical conductance methods.

The accuracy of optical methods is relatively low, especially for thin biofilms, but this method is applicable for most bioreactors. The volumetric displacement method is simple to apply but also provides low accuracy. The electrical conductance method provides high precision but is limited to metal substratum. The thermal resistance method

is simple but has been mainly used for glass slide reactors (Peyton et al. 1995, Lazarova et al. 1995).

All the methods mentioned above are difficult to measure the biofilm growth continuously. *In-situ* biofilm growth monitoring and control requires no disturbance of the system. Therefore, an alternative method to determine the biofilm thickness *in-situ* was investigated in this project by measuring the pressure drop across hollow-fiber bioreactors. For a fixed bed reactor with biofilm attached to particle surfaces, the pressure drop was used to estimate the growth of cells by Kim and Chang (1986). Deront et al. and his colleagues conducted research to determine biomass growth by monitoring the pressure drop in a concurrent biofilter that involved two-phase flow (Deront et al. 1998). However, the pressure drop has never been used to monitor biofilm growth in hollow fiber reactors.

2. 2 Objective and Specific Aims

In this study, a hollow fiber membrane bioreactor (HFM) system was utilized with circulating bacteria cells to stimulate the growth of a biofilm. The pressure drop was utilized to estimate biofilm formation and thickness. As a major part of the study, the Hagen-Poiseuille pressure drop correlation was studied for applicability to the HFM. The major objective of the study was to predict the biofilm thickness by measuring the pressure drop across the HFM and correlating with the Hagen-Poiseuille law. The major objective was accomplished following completion of the following three specific aims.

2.2.1 Specific Aim #1: Assess usability of Hagen-Poiseuille law for flow in HFM.

Liquid flow circulated through the HFM unit and experiments were conducted to measure pressure drop across the HFM unit at different flow rates. Pressure drops were also calculated using the Hagen-Poiseuille law for different flow rates. Experimental results were compared to calculated results for assessing the validity of using the Hagen-Poiseuille law.

2.2.2 Specific Aim #2: Optimize HFM system to enhance biofilm thickness predictability.

The HFM was modified to enhance the accuracy of using the Hagen-Poiseuille law for predicting inner fiber diameters and hence the biofilm thickness. Different fiber systems were designed and studied. Pressure drops through fibers were measured and inner diameters of fibers were predicted. The predictions from experimental data were compared to known fiber diameters.

2.2.3 Specific Aim #3: Prediction of biofilm thickness.

Bacterial cells were cultured and circulated to stimulate biofilm formation. Pressure drops across fiber systems were measured. The Hagen-Poiseuille equation was applied to predict biofilm thickness and the prediction of biofilm thickness was examined by comparison with visual evidence.

CHAPTER 3

ASSESS USABILITY OF HAGEN-POISEUILLE LAW FOR FLOW IN HFM

The primary purpose of Specific Aim #1 was to test the validity of using the Hagen-Poiseuille equation for the flow through the HFM unit. Measurements of the pressure drop across the HFM unit and other fiber systems were conducted and results were compared with calculations based on the Hagen-Poiseuille law.

3.1 Hagen-Poiseuille Law

The Hagen-Poiseuille law is an equation that describes the behavior of flow in a single cylindrical tube. The volumetric flow rate and the forces that cause the flow are associated in the law. The Hagen-Poiseuille law (Bird et al., 1960) is:

$$Q = \frac{\pi (P_0 - P_L) R^4}{8 \mu L} \tag{3.1}$$

where Q is the flow rate through a single tube, R is the inner radius of a single tube, μ is the viscosity of fluid, and L is the length of tube. For the HFM unit, Q equals the total flow rate divided by the number of fibers N_T:

$$\frac{Q}{N_T} = \frac{\pi (P_0 - P_L) R^4}{8 \mu L} \tag{3.2}$$

The assumptions for application of the Hagen-Poiseuille law are listed below:

a. The flow is laminar.

b. The density of flow is constant (incompressible flow).

c. The flow is at steady state.

d. The fluid is Newtonian.

e. The fluid behaves as a continuum.

f. End effects of the tube are neglected.

g. There is no slip at the wall, which means velocity of flow at the wall equals zero.

3.2 Materials and Methods

3.2.1 Experimental set up and operation with HFM

The HFM (Minntech, Fiberflo®, Minneapolis, Minnesota) is a fiber unit containing 1000 polypropylene fibers with ID of 210±10 μm. The wall thickness of each fiber is 27±3 μm. The fibers are glued together and encapsulated in a cylindrical plastic tube with caps on both ends.

The HFM reactor system was connected to a 500 ml Erlenmeyer flask for circulating water through the HFM as shown in Figure 3.1. Tygon plastic tubing with inner diameter of 1/8" and 1/16" wall thickness was used to transport the water. Between the HFM system and flask outlet was a pump and a liquid flowmeter. Water was pumped out of the flask to the liquid flowmeter by a peristaltic pump. The tubing on the outlet of the flowmeter was connected to the HFM system. Two three way valves (Cole Parmer, Cat # P-30600-10) were used for the connection of tubing and the HFM unit. A differential pressure transducer (Validyne Engineering Corp., DP15, Northridge, CA)

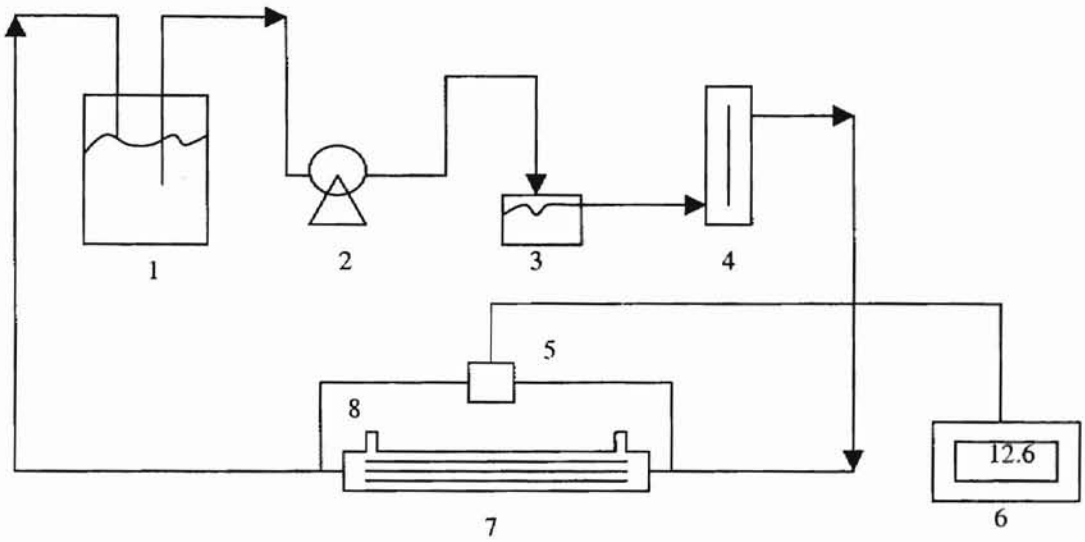

Figure 3.1 HFM reactor system. Water was pumped out of the flask (1) by a peristaltic pump (2) to the liquid flowmeter (4) and then passed through the hollow fiber membrane bioreactor (HFM) unit (7) that has two gas inlet and outlet (8), finally circulated back to the flask. A pulse dampener (3) was used to reduce the pulsing caused by the pump. A differential pressure transducer (5) was utilized for ΔP measurement. A cable connects the pressure transducer to a digital displayer (6).

was connected to both ends of the HFM system by two pieces of 1/16" ID Tygon tubing. Two fittings with one side a male luer lock and the other side a 1/16" hose barb (Cole Parmer, Cat # P-30504-00) were used to connect the tubing to the pressure transducer. A cable was used to connect the pressure transducer to a digital displayer (Validyne Engineering, CD379, Northridge, CA). The whole system was put into an incubator at 30°C (VWR Scientific, Model 535, West Chester, PA).

For each experiment, the pump was turned on and water started to circulate through the entire system. The flow rate was adjusted by the pump. Pressure drops across the HFM unit were read from the digital displayer and recorded at flow rates varying from 0 to 70 ml/min.

During the initial experiments, unstable pressure drop readings occurred. A range of ±12 mmHg was caused by pulsing of the peristaltic pump. In order to get a more stable and accurate reading, a pulse dampener was added to the system. The pulse dampener was placed between the pump and the liquid flowmeter.

The pulse dampener was made with a cylindrical Plexiglas tube sealed both on the top and at the bottom with a sheet of Plexiglas (6 cm OD) using glue. The height of the dampener is 6 cm, the dampener OD is 6 cm, and the wall thickness of the Plexiglas tube is 3 mm. Two holes were placed on the pulse dampener. One hole was at the top and the other hole was on the side. Water flowed into the pulse dampener through the top hole and flowed out the side hole. The pressure drop fluctuation was reduced to ±1 mmHg.

3.2.2 Calibration of liquid flowmeter and pressure transducer

Both the flowmeter and pressure transducer were periodically calibrated. To calibrate the flowmeter, water passed through the flowmeter and was collected in a volumetric flask. The reading on the flowmeter was recorded. The volume of water collected in the volumetric flask for one minute was recorded. The standard calibration curve is shown in Figure 3.2.

To calibrate the pressure transducer, nitrogen was used to pressurize the transducer and a manometer at the same time. The valve on the tank was adjusted to achieve different pressures. The reading on the digital displayer was adjusted to the same value on the manometer. The accuracy of the transducer is 1 mmHg.

3.2.3 Analysis of single tube

Since the Hagen-Poiseuille equation describes flow in a single tube, a piece of 1/16" ID Pharmed tubing (Cole Parmer, Cat # P-06484-04) with lengths of 23 cm was assessed with regards to experimental pressure drops. The experimental set up was the same as for the HFM unit. In this experiment, the HFM unit was replaced by the tube.

However, fittings that connected the single tube to the system were different from those for the HFM unit. Two 1/16" T-shaped stainless steel fittings (Cole Parmer, Cat # P-03301-18) were used for the connection. The experimental pressure drops were compared with predictions from the Hagen-Poiseuille law.

3.2.4 Effects of fittings

The HFM unit was removed from the system and the two three-way valves were

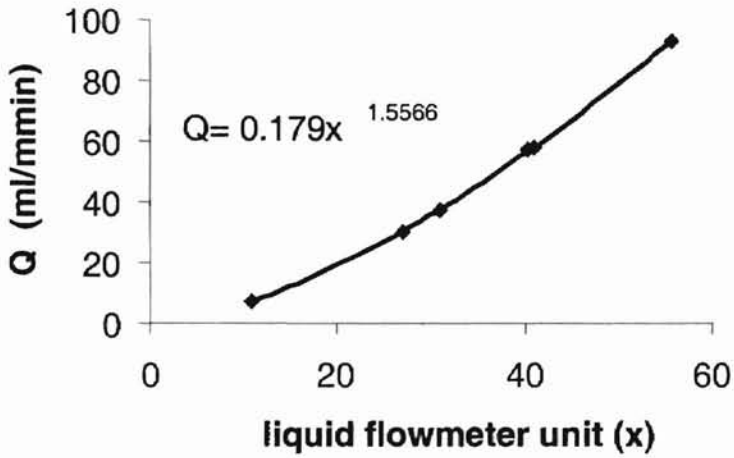

Figure 3.2 Liquid flowmeter calibration curve. Water at 30 °C circulated through a flowmeter. The flow rate was recorded for the corresponding flowmeter unit.

connected together. The pressure drop across the fittings at different flow rates was measured to assess the effects of the fittings alone on the pressure drop. Comparison was made between the pressure drops with and without the HFM unit. The experimental operation was the same as described in section 3.2.1.

3.2.5 Effects of pumps

In order to assess the effects of pumps, such as pulsing vs. non-pulsing on the pressure drop, three different pumps were assessed: peristaltic pump (Masterflex 7520-50, Barrington, IL), syringe pump (Cole Parmer, Cat # P-74900-10), and gear pump (Micropepump 000-305, Vancouver, WA). The peristaltic pump was originally used in the experiments. For the syringe pump, water was filled in a 50 ml syringe and the flow rate was set to the desired flow. The pressure transducer was connected to the HFM unit as before. Water was pumped through the HFM unit and the pressure drop was measured at flow rates between 0 and 45 ml/min in increments of 5 ml/min. Three different connections were used for the gear pump by changing the inlet and outlet tubing sizes to the HFM unit as follows:

a. 1/16" ID tubing inlet and 1/8" ID tubing outlet;

b. 1/16" ID tubing inlet and 1/16" ID tubing outlet;

c. 1/8" ID tubing inlet and 1/16" ID tubing outlet.

The effects of these different connections on the pressure drop were studied.

3.2.6 Effects of viscosity

In the experiments mentioned above, water was utilized. In order to check the effects of viscosity on the pressure drop according to the Hagen-Poiseullie law, water was replaced by 95% air and 5% CO_2 gas mixture. The viscosity of gas is 0.00018 g/cm s. The gas mixture was applied to the single tube described in Section 3.2.3 with a length of 143.5 cm. A digital gas flowmeter was applied to measure the flow rate. The gas flow rates ranged from 0 to 431 ml/min. For this study, the gas was not circulated.

3.3 Results and Discussions

3.3.1 Analysis of HFM unit

For water flow through the HFM unit, the experimental results showed that pressure drop across the HFM unit was much larger than the calculated pressure drop from the Hagen-Poiseuille equation as shown in Figure 3.3. The fiber inner diameter provided from the manufacturer is 210±10 μm. Both the highest and lowest ID limits were used to calculate the pressure drop to provide bounds for the predicted values. In general, the experimental values were twice the theoretical values. However, the relationship between the pressure drop and flow rate was linear, as expected from the Hagen-Poiseuille law. Moreover, the slope of the pressure drop (ΔP) versus flow rate (Q) varied with each run. Thus, there was no consistency in the results. In some cases, the pressure drop increased suddenly without any noticeable changes in the experimental procedures.

When evaluating the usability of the Hagen-Poiseuille law to the HFM unit

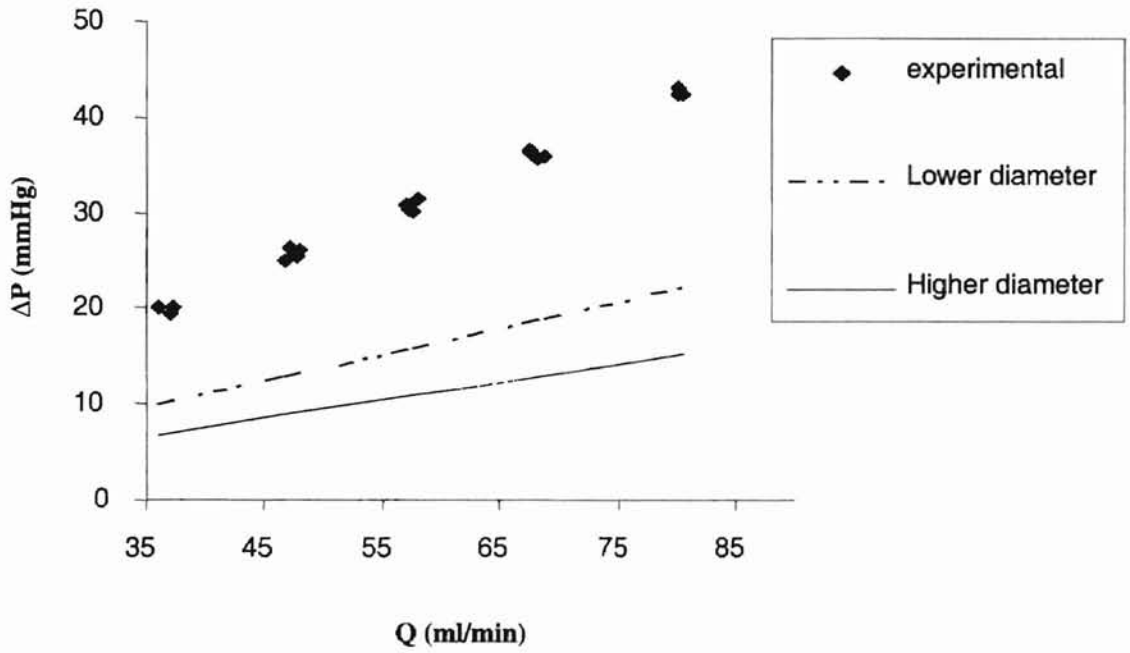

Figure 3.3 Pressure drop through the HFM unit. The Hagen-Poiseuille law was used to calculate ΔP based on the fiber size of the HFM unit. The fiber size was 210 ± 10 μm, where the lower diameter limit is 200 μm and the higher diameter limit is 220 μm. Pressure drops were measured at flow rates ranging from 35 to 80 ml/min at 30 °C.

experiments, the assumptions for this law were examined, since there was disagreement between the law and the experimental results. For this study,

1. The water is a Newtonian fluid.
2. The density of the water is constant since the temperature is constant in the incubator.
3. The liquid behaves as a continuum in the fibers and there is no slip at the wall.
4. The flow is laminar, since the Reynolds number is much lower than 2100.

   The Reynolds number is calculated according to

$$R_e = \frac{4Q\rho}{\pi D\mu} = \frac{4}{\pi}\frac{\left(\frac{80}{1000} ml\ \min^{-1}\right)\left(\frac{1\min}{60s}\right)\left(1.00\frac{g}{cm^3}\right)}{\left(210\mu m\right)\left(0.0085\frac{g}{cm\ \ s}\right)} = 9.52 < 2100 \qquad (3.3)$$

5. And the tubing is long enough for flow to be a fully developed with a parabolic profile. This was confirmed since $L \gg L_e$ where L_e is the length of the region in which flow is fully developed and is calculated according to

$$L_e = 0.035DR_e = 0.035 \times 0.021\ \text{mm} \times 9.52 = 0.0070\ \text{mm} \qquad (3.4)$$

With the above valid assumptions, the Hagen-Poiseuille law should agree well with the experiments. However, experiments showed disagreement. In the Hagen-Poiseuille equation, there are five variables involved that affect the value of the pressure drop (ΔP). These parameters are flow rate (Q), inner diameter (ID) of fibers, length of fibers (L), viscosity (μ), and number of fibers (N_T) in the HFM unit. Besides the factors

that appeared in the equation, there are two other possible factors that may affect the pressure drop: end effects caused by fittings that connect the HFM unit to the system and flow distribution throughout the HFM unit. These factors were examined by individual experiments as previously described in section 3.2.

With regards to Q, the flowmeter reading values were recorded and Q was calculated from the calibration curve. In order to make sure that Q utilized in the Hagen-Poiseuille law was the actual flow rate, the liquid flowmeter was recalibrated periodically. The calibration results were always consistent. Thus Q was not the cause for the higher ΔP compared to the theoretical ΔP.

The length of the fibers was measured as 12.5 cm. The inner diameter of fibers provided from the manufacturer is 210±10 μm. To confirm the ID, pictures of both ends of fibers were taken by a light microscope as shown in Figure 3.4. The measurement from the picture showed the fiber's ID ranging from 206 to 213 μm.

Therefore, evidence showed that the ID of fibers, length of fibers, flow rate and pressure drop reading were not the reason for the experimental deviation from the theory. The viscosity of the fluid, end effects caused by fittings, and flow distribution were possible reasons for the higher ΔP. These parameters are discussed in more detail below later this chapter.

3.3.2 Analysis of single tube

Experimental result showed that when water flowed through a single tube, the relationship between ΔP and Q was still much higher than theory as shown in Figure 3.5. The deviation between the experimental ΔP and theoretical ΔP became larger as Q

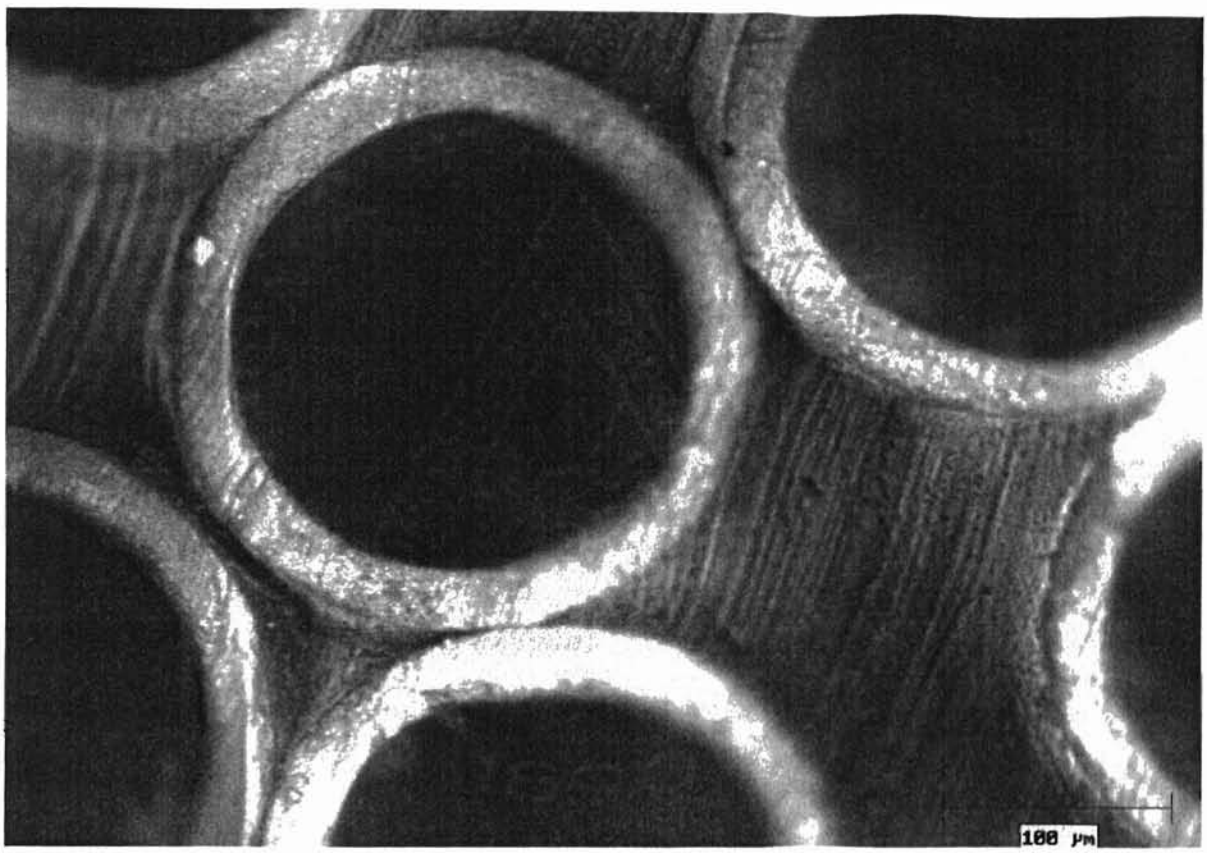

Figure 3.4 Image of end of HFM unit. Inner diameter of fibers of the HFM unit was measured using a light microscope to compare with the value from the manufacturer.

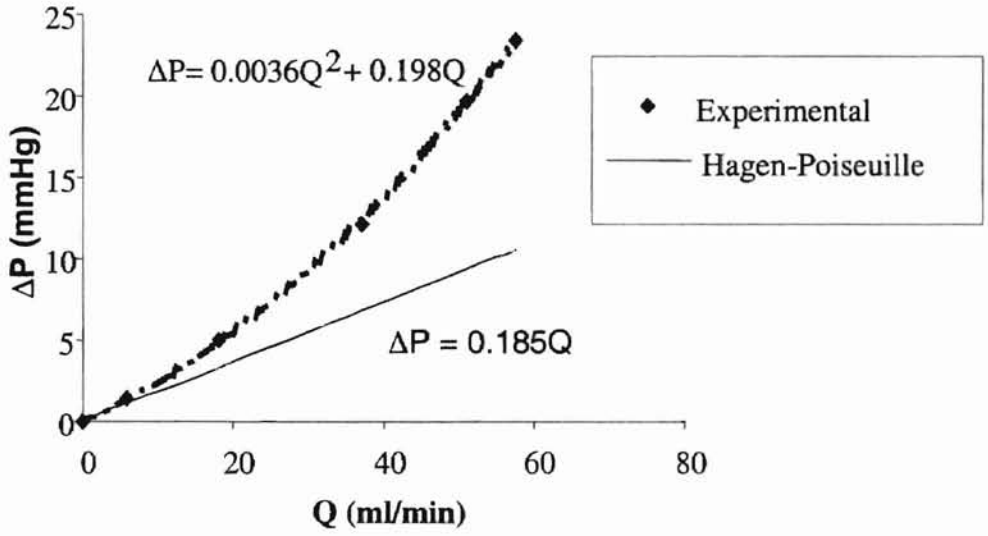

Figure 3.5 Pressure drop across a single tube. The pressure drop across a 1/16" ID tube was measured at different flow rates ranging from 0 to 60 ml/min. Water flowed through the 23 cm long tube at 30 °C. The predicted ΔP according to the Hagen-Poiseuille law is shown.

increased. However, unlike flow through the HFM unit, the relationship between ΔP and Q was not linear but a 2nd order relation. Moreover, the experiments showed that the results were consistently predictable. The 2nd order relationship between the pressure drop and flow rate was indicative of significant entrance and exit effects as well as tube expansions and contractions. This pressure drop or head loss for such effects is a function of the square of the velocity (Bober et al., 1980),

$$h_{L,fitting} = C\frac{V^2}{2g} \qquad (3.5)$$

Since Q = AV, the head loss or pressure drop caused by end effects is second order in Q. According to the Hagen-Poiseuille law ΔP is first order in Q. The conclusion was made that for the single tube, two parts contributed to the pressure drop: the tube itself and end effects (such as the fittings, contraction and/or expansion). Thus ΔP is related to Q by

$$\Delta P = AQ + BQ^2 \qquad (3.6)$$

The 1st order term is the contribution by the tube itself and the 2nd order term is by the end effects. For a Newtonian fluid flow across a single tube, the pressure drop caused by the tube alone obeys the Hagen-Poiseuille law. Therefore, A should be equal to $(8\mu L/\pi R^4)$.

When water flowed through the 1/16" single tube from a 1/8" Tygon tube, there was a compression of flow from a larger cross-section area to a smaller one. Similar geometry changes resulted in expansion at the outlet. Thus, entrance and exit effects are likely to contribute. The experimental curve showed a 2nd order correlation with Q (see

Figure 3.5). The coefficient of the first order term of the experimental curve is 0.198, the calculated Hagen-Poiseuille value is 0.185. Thus, there is good agreement. When the tube contribution to the experimental pressure drop value is used to predict the inner diameter, a value of 0.156 cm ID is obtained. This agrees well with the actual ID of 0.159 cm. Since R is related to $\Delta P^{1/4}$, the error in calculating R from ΔP measurements is even smaller compared to the error in ΔP measurements. In summary, the above results showed that the Hagen-Poiseuille law is applicable for a single tube to predict the ID of the tube. However, the end effects must be accounted for.

3.3.3 Effects of fittings

In order to find out whether the measured ΔP was only due to the HFM unit, the effects of fittings were examined. Results showed that no significant ΔP appeared when water flowed only through the two connected fittings. There was no noticeable change in ΔP with any change in the liquid flow rate. This result correlated very well with the linear relationship between ΔP and Q in the HFM unit because the effects of fittings should provide a second order contribution to the pressure drop. Thus, evidence suggests that when water flowed through the HFM unit, fittings were not one of the factors that made ΔP higher than theoretical predictions.

As previously observed with the single tube, as water flowed through fittings from a 1/8" tubing to a 1/16" tubing, the fittings contributed to the pressure drop, with ΔP proportional to the square of the flow rate. However, when water flowed into the HFM units (composed of 1000 tubes), the fittings did not contribute since ΔP across the fiber is likely much greater than across the fittings.

3.3.4 Effects of pumps

Another hypothesis for the discrepancy between the experimental and theoretical ΔP across the HFM unit was the pulsing caused by the peristaltic pump. Two other pumps were applied to the system to assess the hypothesis. Experiments showed different results for different pumps as seen in Figure 3.6. The system with the syringe pump had the lowest pressure drop across the HFM unit. When the gear pump was placed into the system with varying inlet and outlet tube sizes, different results were observed. Pressure drops were lower if the tube size was bigger (both inlet and outlet is 1/8" ID). With 1/16" inlet and 1/16" outlet tubing, pressure drops were the highest. When the gear pump was connected to 1/16" inlet and 1/8" outlet, pressure drops were between the other two different sized tubes. Compared to the other two pumps, the pressure drop across the HFM unit with a peristaltic pump was between the highest and lowest values. However, ΔP was linearly related to Q in all experiments, showing that fittings did not contribute to the higher experimental ΔP as compared to predictions. The experiments showed that the type of the pump affected the pressure drop across the HFM unit. Different results indicated that flow conditions varied with different pumps.

The syringe pump provides flow that is more evenly distributed because there is no pulsing. In this case, the experimental ΔP was much closer to the theoretical value than other situations. For the peristaltic pump, pulsing of flow may change the flow conditions, then making ΔP higher. When the pump removed water from flask, pulsing caused uneven flow. When water flowed into the HFM unit from the connecting tubing, water may not have been well distributed. The thousand tiny fibers were distributed in a module that has a cross section area around 2.3 cm^2. If water was well distributed

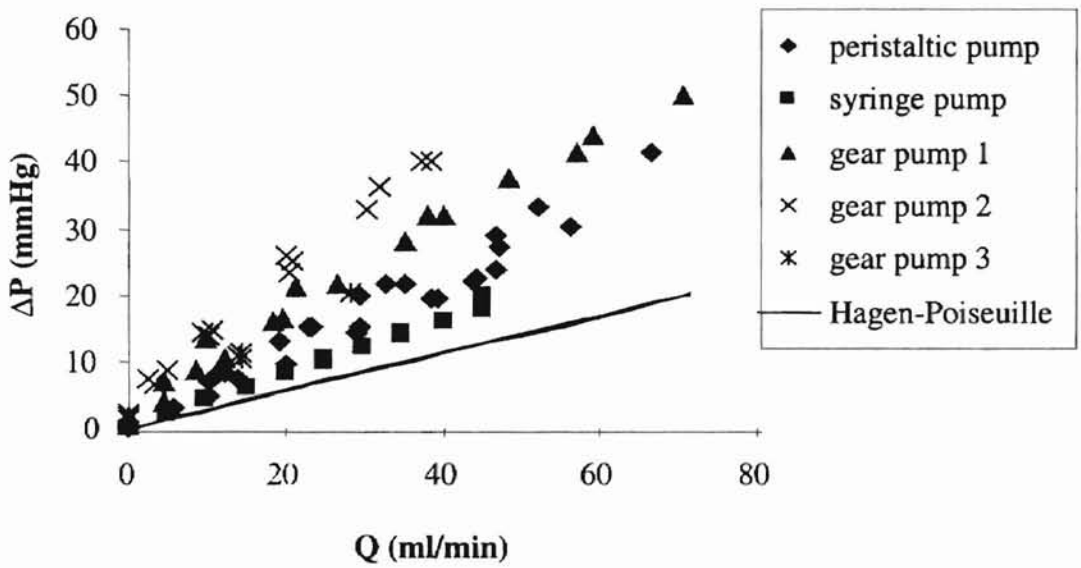

Figure 3.6 Pressure drop across the HFM with different pumps. Three different pumps were used to assess the effects of pumps on ΔP across the HFM at various flow rates. For the gear pump, three different size connections were used. Gear pump 1 has inlet 1/16" and outlet 1/8" size tubing; Gear pump 2 has inlet and outlet 1/16" size tubing; Gear pump 3 has inlet and outlet 1/8" size tubing. Water was used at 30 °C for all experiments.

before flowing into the fibers, all 1000 fibers would be used. However, the end caps of the HFM module are so short that water may not have passed through each fiber. Thus, the number of fibers being used would not be 1000, this causing the flow rate through each fibers to be higher, which in turn would cause the discrepancy of ΔP between the theoretical value and experimental.

3.3.5 Effects of viscosity

In order to check whether the viscosity was contributing to the higher experimental ΔP, both gas and liquid flow were assessed. When gas flowed through the single tube, the results showed that the Hagen-Poiseuille law agreed with experiments very well as shown in Figure 3.7. The experimental ΔP was very close to the theoretical value and also the relationship between ΔP and Q was linear as expected. There were no fitting effects or contraction problems. When the experimental ΔP was applied to the Hagen-Poiseuille law, the predicted tube ID was 0.160 ± 0.0011 cm while the actual value is 0.159 cm. The prediction of ID was excellent. Also, as mentioned in Section 3.3.2, when water flowed through the single tube, the prediction of ID was also very close if the part contributed by the tubes itself was only utilized. Therefore, the Hagen-Poiseuille law is effective in predicting the ID of single tubes, and the viscosity is not the factor that affects the experimental ΔP.

3.4 Conclusion

Experiments showed that the experimental ΔP across the HFM unit was higher than the calculated ΔP according to the Hagen-Poiseuille law. All assumptions for the law

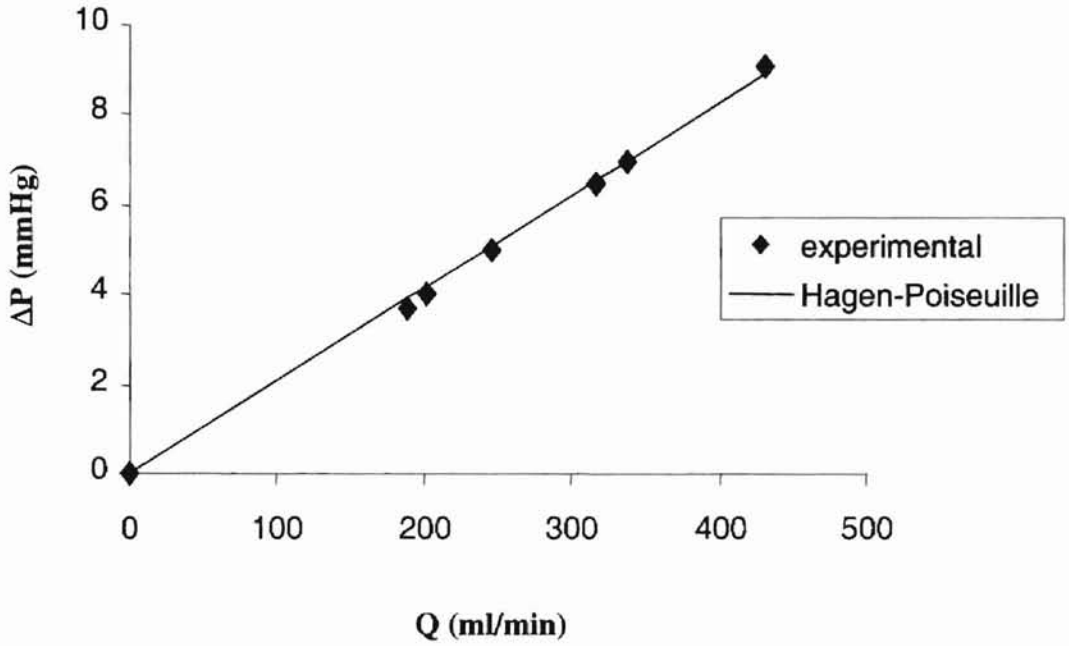

Figure 3.7 Pressure drop across single tube with gas flow. Nitrogen gas was purged through a piece of 1/16" ID tube and L = 143.1 cm. Pressure drop was measured at flow rates ranging from 0 to 450 ml/min at 30 °C to assess the effects of viscosity.

appeared valid for the experiments, if end effects were neglected. A linear relationship between ΔP and Q demonstrated there were no effects of fittings. Analysis of a single tube with gas flowing through showed that the Hagen-Poiseuille equation agreed well with the experimental value. For liquid flow through the single tube, the experimental ΔP was much the higher than theoretical value. Moreover, the relationship involved a 2^{nd} order term. The result indicated end effects contributed to the ΔP. If the end effects were accounted for, the Hagen-Poiseuille law agreed well with experiments. Therefore, the conclusion was made that the Hagen-Poiseuille law should work for the HFM unit. The higher experimental ΔP was likely the result of flow distribution and number of fibers being used. The poor flow distribution caused the number of the effective fibers to be smaller than the total number of fibers, which resulted in a higher ΔP across the HFM unit.

The solution of the problem was to design a HFM system that has a distance long enough for flow to distribute well before flowing into the fibers. This would improve the effective usage of fibers and therefore reduce the experimental ΔP across the HFM unit.

CHAPTER 4

OPTIMIZATION OF FIBER SYSTEM

In the last chapter, the results showed that the flow distribution of liquid in the HFM unit may have led to higher experimental ΔP as a result of not all the fibers being utilized. In order to reduce or eliminate this problem, the HFM unit was modified. In addition, new fiber units were designed for convenience in working with the cell experiments described in Chapter 5. Experiments were again performed to compare experimental ΔP to theoretical predictions.

4.1 Materials and Methods

4.1.1 Experimental set up and operation

The same experimental system with a peristaltic pump, as described in Chapter 3, was used. The peristaltic pump was chosen for convenience with the cell experiments described in Chapter 5. However, different fiber units (including the HFM unit) were used to assess ΔP. As stated before, water circulated through the system and the pressure drop was measured and recorded at different flow rates. Three sets of experiments were conducted:

1. Pressure drops were measured at flow rate ranging from 0 to 80 ml/min at 30°C. Experimental pressure drops were compared with predictions from the Hagen-Poiseuille equation.

2. Since cell culture experiments were designed to last at least 48 hrs, a stable pressure transducer reading is essential. In order to make sure that the baseline of the pressure transducer reading would not fluctuate with time, the stability of the pressure transducer was investigated. At a flow rate of 35.7 ml/min and 30°C, the pressure drop across the HFM unit was measured and recorded for 24 hrs.
3. To assess repeatability within an experiment, flow rate was increased from 0 to 80 ml/min and then decreased to 0 ml/min at 30°C. This procedure was repeated one more time and pressure drops across the HFM unit at different flow rates were measured. Experimental and theoretical ΔP values were compared.

4.1.2. Modified HFM unit.

HFM units were ordered without end caps that originally were glued to both ends of the unit. Two Plexiglas chambers were made to provide a better distribution of flow to the hollow fibers. The dimensions of the chambers are given in Figure 4.1. Each chamber consists of a cylindrical tube formed drilled in Plexiglas from one end with a diameter of 17.1 mm and length of 4.5 cm. The tube was as big as the outer diameter of the HFM unit's shell so that the HFM unit without end caps would slide in. An O-ring inside the chamber helped prevent the unit from leaking. Another two holes were also drilled in each chamber for connections. A hole on the top was used to connect to the pressure transducer. This hole was close to the HFM unit so that the ΔP measurement would primarily be attributed to the HFM unit. The other hole was for the liquid flow to

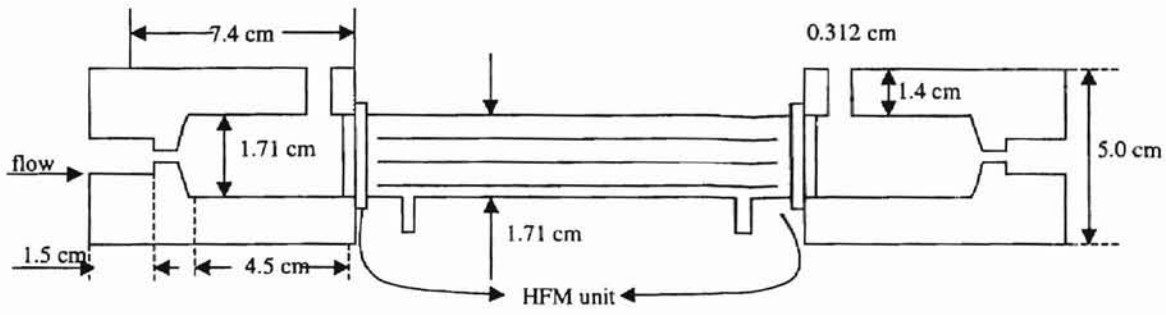

Figure 4.1 Modified HFM unit. Plexiglass chambers were formed to attach to the HFM unit. The holes at the end of the chambers are used to connect to the tube; the holes at the top of the chambers are for the connection to the pressure transducer.

the HFM unit. Prior to each experiment, bubbles were removed from the HFM unit and chambers to ensure effective flow through each of the fibers.

4.1.3 New fiber units

In order to verify the estimation of the biofilm thickness using experimental ΔP and the Hagen-Poiseuille law, optical confirmation had to be provided. For experiments of culturing cells as describes in Chapter 5, comparison of the actual biofilm thickness with the prediction of the biofilm thickness is essential. However, from the picture taken by light microscope described in chapter 3 (Figure 3.4), using a light microscope was not feasible since the inside of the fibers were too dark to measure the biofilm thickness. It was difficult for light to go through the whole HFM unit because of the length of the fibers. This would be a major disadvantage for later studies of biofilm formation. In order to determine the ID of fibers and hence the biofilm thickness in later research, the fibers in the HFM unit had to be cut into short pieces. However, the design of the HFM unit made this difficult. In order to get a clear image inside the fibers, new fiber units were made.

Tube bundles made of different materials and sizes were cut at certain lengths and glued together at both ends to form the new fiber unit. The radius and number of tubes was determined by ensuring that the change of ΔP would be measured with a significant biofilm growth according to

$$\Delta P_i = \frac{8\mu LQ}{\pi N_T R_i^4} \tag{4.1}$$

The relationship between changes in the tubing ID and the associated change in ΔP is shown in Figure 4.2 for a flow rate of 30 ml/min, a length of 10 cm, and for 5 or 10

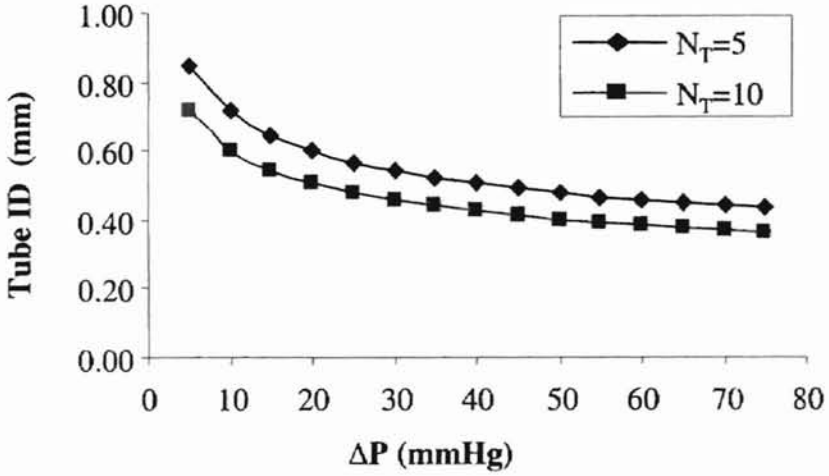

Figure 4.2 Tube ID vs. ΔP. The pressure drop for various tube diameters are shown for Q=30 ml/min as predicted from the Hagen-Poiseuille law. N_T represents the number of parallel tubes, through which liquid flows. Water at 30 °C was assumed as the flowing fluid.

tubes. The viscosity was assumed to be that of water with a value of 0.0085 g/cm s at 30 °C. Figure 4.2 shows that a bundle of ten tubes with ID of 0.50 mm would result in ΔP of 20 mmHg. If a 10 μm thick biofilm formed inside the tube, the ID would change to 0.48 mm and ΔP would increase to 30 mmHg, which would give a noticeable change of ΔP.

Figure 4.3 shows the predicted ΔP with biofilm growth (ΔP_b) relative to ΔP without growth (ΔP_i). For biofilm growth, ΔP is

$$\Delta P_b = \frac{8\mu LQ}{\pi N_T (R_i - t)^4} \tag{4.2}$$

Thus, the ratio is

$$\frac{\Delta P_b}{\Delta P_i} = \left(\frac{R_i - t}{R_i} \right)^4 = \left(1 - \frac{t}{R_i} \right)^4 \tag{4.3}$$

where t is the biofilm thickness and R_i is the inner radius of the fibe.

For cell cultures inside the tube, the material of tubes should be attachable for pseudomonas aeruginosa cells. If the tube is air permeable, the air will help cells growth since pseudomonas aeruginosa is aerobic. Also the materials should be nontoxic to cells. Plastics are the materials that cells have a tendency to grow on. Silicon tubing, polyimide and polypropylene (PP) have been used for cell cultures in literature, especially PP due to its high air permeability. Silicon tubing has an operation temperature at 200 °C, and this property makes it possible for autoclaving.

4.1.3.1 Platinum cured silicon-tubing unit

Platinum cured silicon tubing of .50 mm ID (Cole Parmer, Cat # P-95802-00, Vernon

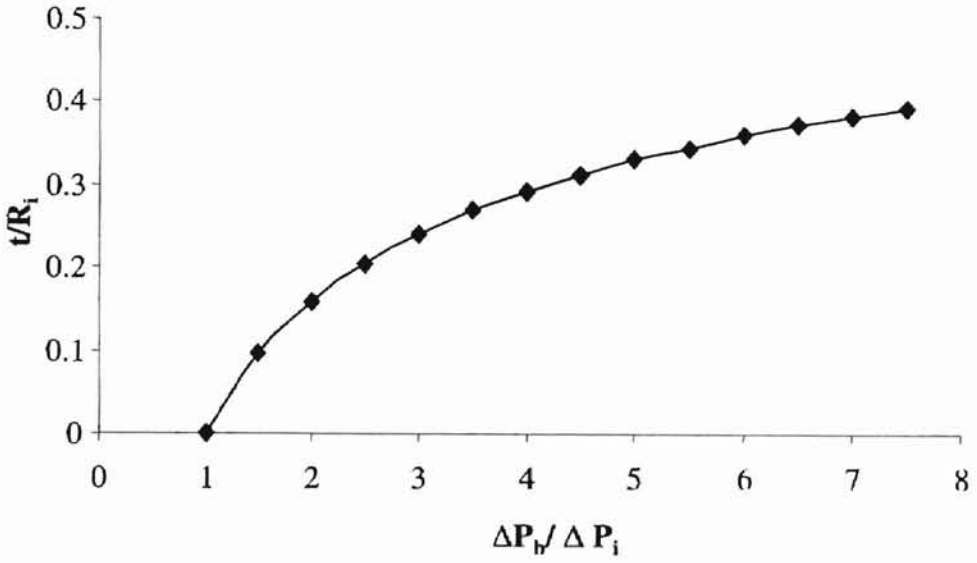

Figure 4.3 Change of ΔP vs. biofilm growth. The pressure drop with biofilm growth (ΔP_b) is shown relative to the pressure drop with no growth (ΔP_i). The bioiflm thickness is t and R_i is the tube inner radius. Simulations are based on equation 4.3.

Hills, IL) cut was into pieces and glued together at the end as parallel tubes using silicone adhesive. Heat shrink tubing (1/4") was placed over both ends of the silicon tube bundles. A heat gun was used to heat the shrink tubing until the heat shrink tubing became tight. The fiber unit ends were connected to the system by two 1/8" unions. Two needles were stuck into the 1/8" Tygon tubing near the exit and entrance of the fiber units. The other ends of each needle were connected to the pressure transducer by 1/16" tubing. Two platinum cured silicon units were made, one with five tubes (N_T=5) and L=13.1 cm, and the other with ten tubes (N_T=10) and L=24.5 cm.

4.1. 3.2 Polyimide tubing and polypropylene tubing unit

The same procedure as described in section 4.1.3.1 was applied to make units of polyimide tubing. The ID of the polyimide tubing is 0.0235", length of unit is 27.4 cm, and number of tubes is 14. For polypropylene tubing, the maximum useable operation temperature is around 120°C. Therefore, the heat gun could not be used to make polypropylene units. A parallel bundle of 12 pieces with length of 14.4 cm of polypropylene tubing were glued together at the end and the ends were inserted into short pieces of 1/8" Tygon tubing. The fiber unit was cured overnight before application. For all fiber units, a small portion of each end was cut to ensure the tubes were not blocked as a result of the glue process.

4.2 Results and Discussions

4.2.1 Modified HFM unit

As shown in Figure 4.4, the experimental ΔP versus Q agreed well with the Hagen-Poiseuille law. The experimental relationship between ΔP and Q was linear, and ΔP versus Q was between the interval of ΔP based on lower diameter and upper diameter limits based on the manufacturer's fiber measurements. The results showed that the HFM modifications improved the HFM unit ΔP predictions dramatically. Compared to the original HFM unit with end caps, the Plexiglas chamber modification allows the water to become well distributed before it flows into the HFM unit. Without the chambers, the water flows into the HFM immediately after flowing out of the fittings (three-way valves). Water passes a 1/8" tubing, through a three-way valve and then into a 14.5 mm ID fiber module in which approximately 1000 small fibers are distributed. The short distance between the end cap and the entrance to the fibers makes it very difficult for the water to evenly distribute so that water could flow through each fiber. This appears to be the reason that the unmodified HFM unit did not provide good experimental agreement of ΔP with theoretical predictions.

Sometimes, especially at the beginning of the experiment using the modified HFM unit, ΔP was much higher than the theoretical value. Therefore, the HFM unit was tipped vertically and tapped. Bubbles came out of the HFM unit exit and ΔP decreased to the right range. Thus, the elimination of bubbles is an extremely important problem that could be caused not only by flow distribution at the fiber ends, but also by the blockage

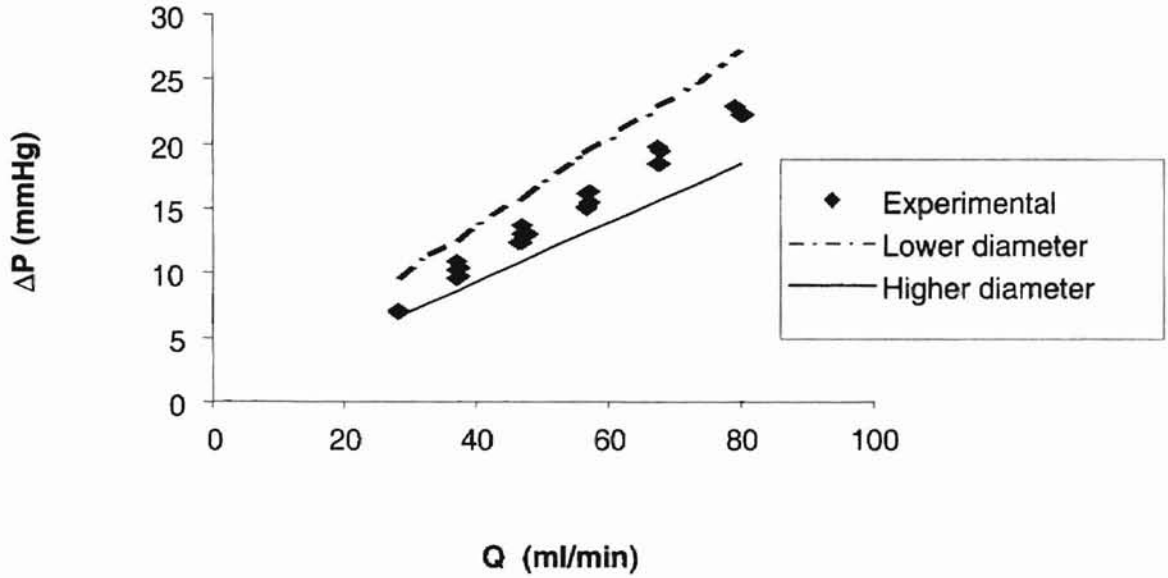

Figure 4.4 Pressure drop across modified HFM unit. When water flowed through modified HFM unit (with chambers on both ends), pressure drop was measured at different flow rates. The water was at 30 °C. The upper and lower limits represent predictions from the Hagen-Poiseuille law for the upper and lower diameter limits.

of the fibers. When water flowed through the fibers, some of the fibers could be blocked because of small particles or air bubbles in the water. The blockage would result in a small decrease in available tubes which would make the experimental ΔP higher than the theoretical value. Therefore, making the HFM unit vertical and tapping the HFM unit could help to push air bubbles and particles out of the fibers.

The stability of the pressure transducer reading is very important for cell culture research. The results showed that there was no noticeable change of pressure drop for up to 24 hrs at a fixed flow rate. Since the reading of the pressure transducer was stable, experiments could be conducted continuously for a long time.

There were some differences of ΔP at a fixed flow rate when Q was increased and then decreased back to the same Q (see Figure 4.5). As the flow rate was increased to 80ml/min and then reduced again, ΔP was lower than the original ΔP, although the difference was not large. After reducing the flow rate, ΔP remained stable. The results suggest that some of the fibers may not have been utilized at the beginning of the experiment that might be caused by a flow distribution problem. Increasing Q to a large flow rate prior to setting the final flow rate helped distribute the flow to the fibers.

4.2.2 Platinum cured silicon tubing unit

When water flowed through the platinum cured silicon unit with N_T=5 and L=13.1cm, the experimental ΔP was very high relative to theory as shown in Figure 4.6. The relationship between ΔP and Q involved a 2nd order relation. Figure 4.6 shows that a second order term contributed to the higher reading of ΔP, which is indicative of the end effects caused by fittings as described in section 4.1.3.1. However, the first order term

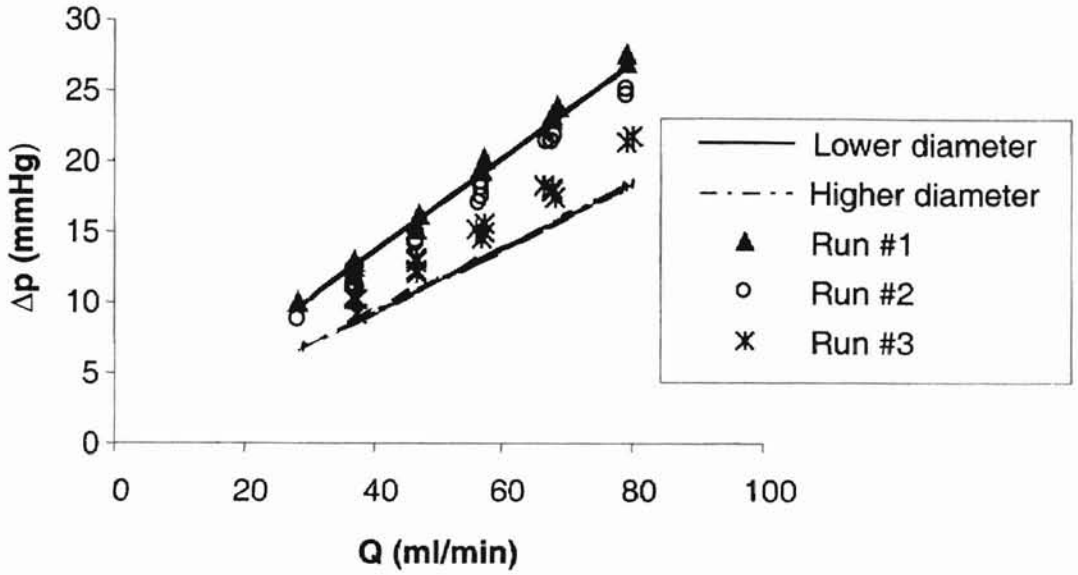

Figure 4.5 Effects of flow rate on pressure drop. Pressure drop was measured across the modified HFM unit (described in section 4.1.2) as a function of flow rate. For run #1, flow was continually increased for each measurement, beginning at 20 ml/min. For run #2, flow was decreased beginning at 80 ml/min. For run #3, flow was increased again, beginning at 20 ml/min. Water was used at 30 °C. The upper and lower limits represent predictions from the Hagen-Poiseuille law for the upper and lower diameter limits.

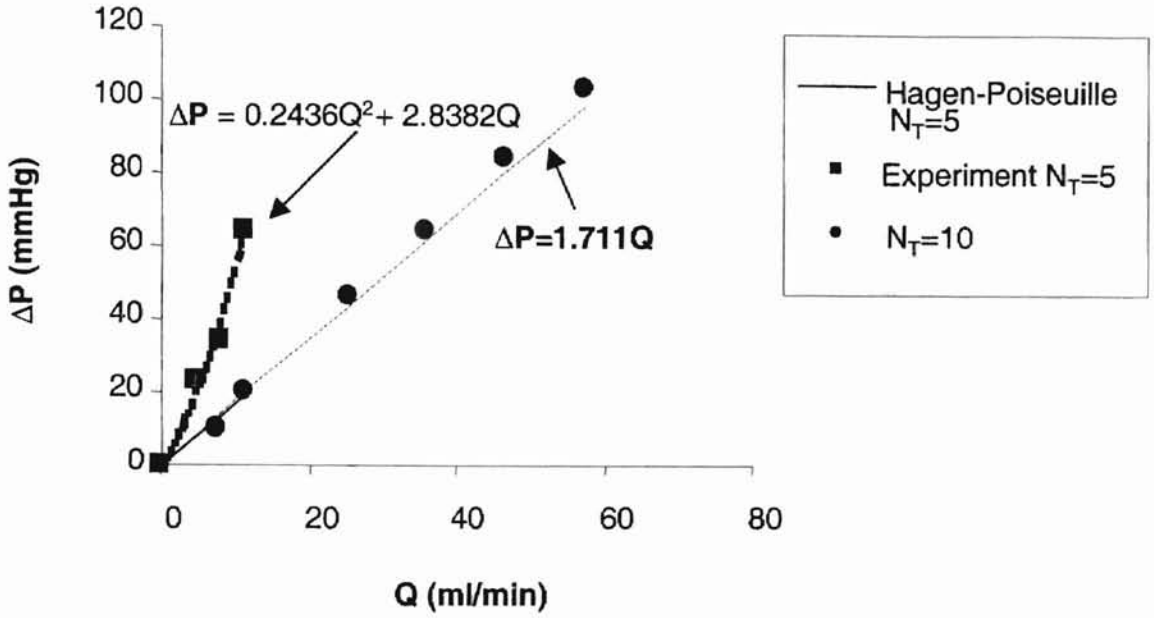

Figure. 4.6 Pressure drop across platinum silicon unit. Water flowed through a platinum silicon unit with five tubes at 30 °C, the pressure drop was measured at different flow rates. The Hagen-Poiseuille law gives $\Delta P=1.67Q$. Experimental curve fits are shown for N_T values of 5 and 10.

coefficient was 2.84 was larger than that calculated from the Hagen- Poiseuille law, which was 1.67. This may be the result of ineffective usage of tubes caused by flow distribution problems. Increasing the number of tubes helped reduce the disagreement between the experimental ΔP and the theoretical value. A platinum cured silicon unit was made with $N_T = 10$ and $L = 24.5$ cm. The results in Figure 4.6 show that the experiment and the theory agree very well. The relationship between ΔP and Q is linear and the experimental ΔP was very close to the predicted value according to the Hagen-Poiseuille law. Thus, increasing the number of tubes from 5 to 10 helped to reduce the end effects. One method to reduce potential errors in ΔP measurements would be to increase the length of tubes. This would reduce the contribution of entrance/exit effects on the measured ΔP.

4.2.3 Polyimide and polypropylene unit

Experiments showed that for the polyimide and polypropylene units, the experimental ΔP versus Q was very close to the theoretical value as shown in Figure 4.7. The slope of ΔP vs. Q for the polyimide unit was 1.735 and theoretical slope was 1.501. This discrepancy may due to the sensitivity of the experimental set up, and the accuracy of tube ID and length measurement. However, as described below, this discrepancy does not drastically affect the prediction of the tube radius based upon the experimental ΔP. For both fiber units, the ten parallel tubes helped reduce potential end effects caused by the fittings. The relationship between ΔP and Q was linear for both units.

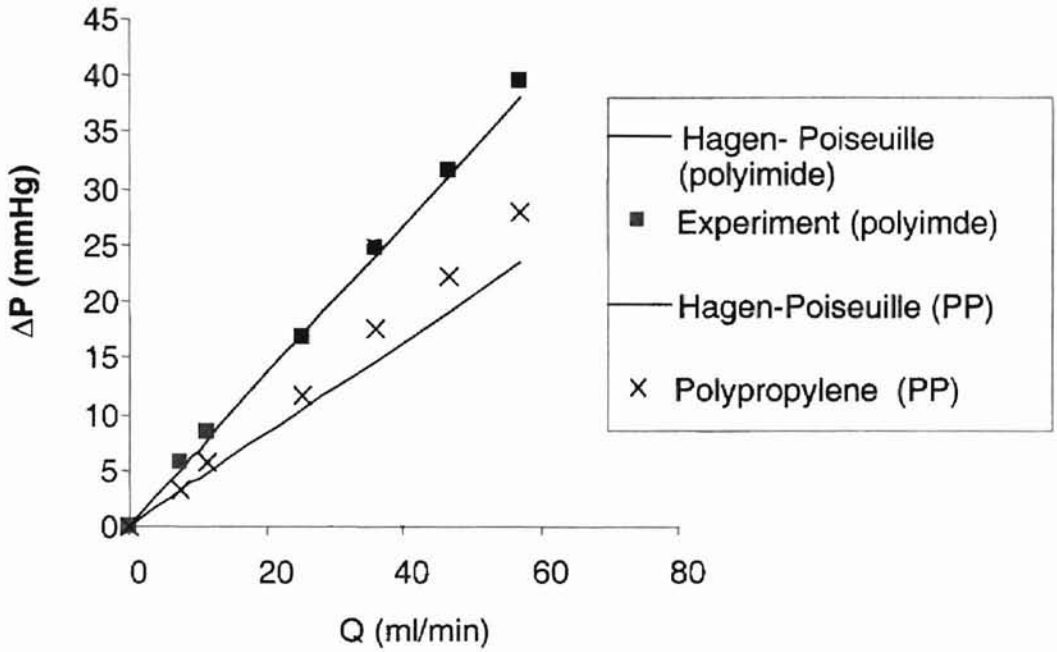

Figure 4.7 Pressure drop through polyimide (N_T=14, L=27.4 cm) and polypropylene units (N_T=12, L=14.4 cm). The experimental relationship between ΔP and Q was measured at different flow rates for water flowing at 30 °C. Predictions are based on the Hagen-Poiseuille law.

4.2.4 Prediction of tube ID based on ΔP

The objective of this research was to determine the biofilm thickness. Therefore, predicting ID of tubes was essential. When using the Hagen-Poiseuille law with experimental ΔP to calculate ID of tubes, R is proportional to $(1/\Delta P)^{1/4}$. Thus, when ΔP was applied for the prediction of ID, the error associated with predicting R was reduced dramatically compared to the error associated with the experimental ΔP.

For the modified HFM unit and new fiber units, Figure 4.8 shows the prediction of tube ID for each fiber unit in comparison with the known ID from the manufacturers. The prediction of tube ID was reasonably accurate and the relative errors were within 4%.

4.3 Conclusion

For the original HFM unit, the flow distribution was a major problem for obtaining an accurate ΔP. After modification, water was well distributed before flowing into the HFM unit. For both modified HFM unit and new fiber units, experimental ΔP matched well with theoretical ΔP predicted from the Hagen-Poiseuille law. The prediction of tube ID was quite accurate and results showed that the relative error was within 4%. The accurate prediction of ID demonstrates the feasibility of using the Hagen-Poiseuille law for predicting the biofilm thickness inside a fiber by noting the change in ID.

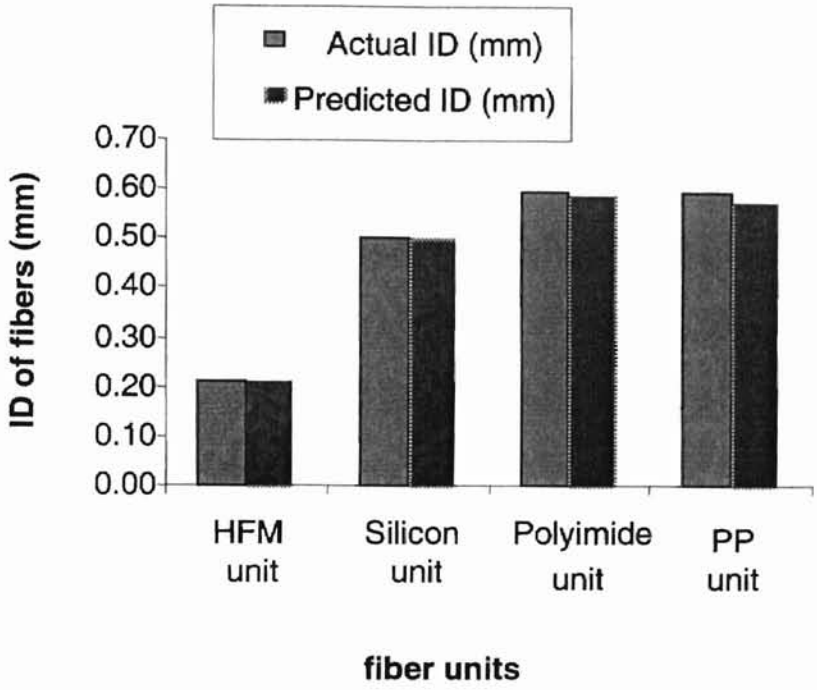

Figure 4.8 Prediction of ID for fiber units. The ID of several units were predicted by the Hagen-Poiseuille law and experimental data and were compared with the actual ID. The HFM unit was described in section 4.1.3.1, and the silicon, polyimide and PP (polypropylene) units were described in sections 4.1.3.2 and 4.1.3.3.

CHAPTER 5

PREDICTION OF BIOFILM THICKNESS

Results of Chapter 4 showed that the Hagen-Poiseuille equation can successfully predict the fiber ID if flow is well distributed and effects of fittings are negligible or are accounted for. For the modified HFM and the homemade tube units with $N_T \geq 10$, the ID can be estimated quite accurately. Therefore, the Hagen-Poiseuille law can theoretically be utilized for predicting the biofilm thickness inside a fiber.

5.1 Materials and Methods

5.1.1 Fiber units

Five modified HFM units with chambers and four homemade fiber units were used for cell culture experiments to assess biofilm growth.

a. Five new HFM units (Fibercor, Mintech) connected with chambers were used. One unit was reused following sterilization to assess reusability.
b. Two platinum cured silicon units were used with 0.5 mm ID. The first unit had ten tubes that were 24.6 cm long. The second unit had ten tubes that were 25.6 cm long.
c. A polyimide unit was used with 14 tubes, a length of 27.4 cm and an ID of 0.0595 cm
d. A polypropylene unit was applied with 12 tubes, a length of 14.4 cm and an ID of 0.000595 cm.

Complete unit descriptions are given in Chapter 4.

Sterilization was not performed on most units before each experiment. However, sterilization was performed on one HFM unit and the polypropylene unit. Due to the operation temperature of polypropylene, an autoclave procedure could not be applied. 70% ethanol was prepared and transferred into a 500 ml Erlenmeyer flask. The ethanol solution was recirculated in the polypropylene system for one hour. Afterwards, sterile water was recirculated in the system for two hours to rinse out the ethanol residue.

For all HFM units that were not cut to examine the biofilm for visual evidence, sterilization procedures were carried out to kill the bacteria in the HFM unit and clean the system following each experiment. The sterilant (1 ml, Minncare Cold Sterilant, Fibercor, Minneapolis, MN) was mixed with nanopure water in the hood. The solution was pumped into the HFM unit and two three-way valves were used to seal both ends of the inlet and outlet. The fibers remained in contact with the sterilant for 1.5 hours. Afterwards, the sterilant was removed and replaced by nanopure water and circulated through the entire system. This rinsing process was performed at least four times.

5.1.2 Cell preparation

Pseudomonas aeruginosa was utilized for this study since they easily adhere to many surfaces. Pseudomonas aeruginosa is an aerobic and Gram-negative bacterium with a rod shape. The size is around 0.5 -1.0 μm by 1.5 - 4.0 μm. The optimal culture temperature for most strains of Pseudomonas aeruginosa is 37 °C. Pseudomonas aeruginosa biofilms consists of individual bacterial cells embedded in an extra-cellular polysaccharide matrix, which are very homogenous compared to other biofilms.

Suspended pseudomonas aeruginosa in nutrient medium was kindly provided by Dr. Robert Miller at Oklahoma State University. Nutrient medium for pseudomonas aeruginosa was Bacto Luria Broth Miller (Difco Inc. San Jose, CA). The nutritionally rich medium is designed for the growth of pure cultures of recombinant strains. The contents of Luria Broth Miller are:

Bacto Tryptone.....10g

Bacto Yeast Extract..... .5g

Sodium Chloride.....10g

Final pH 7.0 ± 0.2 at 25°C

LB Broth (6.25g) was dissolved in 250ml Nanopure water in a 500ml Erlenmeyer flask. An aluminum paper was used to cover the top of the flask. The flask with medium was autoclaved at 121°C for one hour. After cooling down, the flask was put into the incubator (VWR Scientific, Model 1535) for some time before cells were added.

5.1.3 Scanning Electron Microscopy Examination

Following each experiment, fibers were cut (cross-section) into pieces of 1.5 cm long. Several sections were obtained along the length of the fiber for a better comprehensive idea of bacteria growth along the HFM unit. In general, samples were taken at both ends and at 1/4 length intervals. At each site, ten short pieces around 1cm long were selected randomly for analysis. Images of the tubing were taken without cell exposure as a control. The Scanning Electron Microscope (SEM) examined biofilms using two different sample fixation procedures.

The first procedure involved cryofixation and was used for the HFM units. An electric saw was used to cut both ends of the HFM unit. The fibers were taken out of the plastic shell and cut into pieces of 1.5 cm long by a razor. Afterwards, these short pieces were placed on an aluminum crystostub with silver paint, which supports the sample when it is placed in the SEM. The crystostub was submerged in an -80°C cryofixation unit, then coated with Au/Pd for one minute. The sample was put into the SEM (JEOL JXM 6400) and heated up to -40°C. For this method, the sample was observed at 5 KV and photographed.

The second procedure involved glutaraldehyde fixation and was used for the homemade fiber units. The fibers were cut into pieces of 1.5 cm long with a razor and fixed in 2% phosphate buffered glutaraldehyde for 2 hrs. An empty piece of fiber without bacteria was also cut for the control. The fibers were placed in 0.1M phosphate buffer and washed three times for twenty minutes. The samples were then fixed in 1% phosphate buffer for two hours, then washed with 0.1M phosphate buffer three times for twenty minutes each. The samples sat in the phosphate buffer overnight in a refrigerator. The samples were then repeatably dehydrated three times with an ethanol solution using 50, 70, 90, 95, 100 percent in successive increases. Each step lasted for twenty minutes. The samples were finally dried and placed on an aluminum stub. The samples were put into the SEM and observed at 20 KV (25 KV for control).

5.1.4 Experimental operation

Before each experiment assessing biofilm growth, nanopure water flowed through

the system. ΔP was measured at different flow rates and compared with theoretical predictions to ensure all fibers or tubes were used. Afterwards, water was removed from the system and the nutrient medium was circulated through the system. Different experimental procedures were applied for different fiber units. The primary differences were flow rates, total culture time, and different bacteria solution preparation.

Six runs using the HFM unit were conducted as follows. The cultured cell solution (250 ml) was directly added to the system without additional medium. The flow rate was either 25.4 or 35.7 ml/min. All experiments were conducted for about 48 hours. For one experiment, after a dramatic increment of ΔP was observed, fresh medium replaced the cell suspension and was circulated through the system. All runs were at 37 °C. In only one of the six experiments, the SEM was utilized to examine biofilm growth with cryofixation as described in section 5.1.3.

Three experiments were conducted using two platinum silicon units. The first experiment was conducted by directly added 250 ml of suspended cells with a flow rate of 35.7 ml/min. For the second experiment, the cell solution was prepared as follows. Cell suspension (150 ml) from overnight culture was transferred to a sterilized centrifuge tube. The centrifuge tube was put into a centrifuge (Sorvall RC-5B Refrigerated Superspeed Centrifuge) and was centrifuged at 7000 rpm/min at temperature around 4°C for 14 minutes. The bacteria pellets were transferred into a 250 ml flask with nutrients. Cell pellet was resuspended in the flask and the flask was placed in the system. The cell solution sat still for six hours with the pump turned off prior to circulation. The third experiment was similar to the second experiment. However, cells sat still for 12 hours prior to the circulation. The culture temperature was 30 °C.

The Polyimide unit experiment was conducted as follows. Cell suspension (10 ml) following an overnight culture was transferred to 250 ml fresh and sterilized medium without centrifuging. The solution sat in the fiber unit for five hours prior to the start of the experiment. Then, the cell suspension flowed through the entire system for 22 hours at 30°C. For cell cultures in both platinum cured silicon units and polyimide unit, the gluteraldehyde fixation procedure described in section 5.1.3 of cells was used for photographing the fibers after the experiment.

For polypropylene unit experiments, cells were prepared similar to the polyimide unit. Cells were cultured after placement in the system for eight hours with constant stirring at 35°C. Afterwards, flow was initiated at 35.7 ml/min for 23 hours and then the flow rate was reduced to 11.4 ml/min for 51 hours. All experimental conditions are summarized in Table 5.1. A Ubbelohde viscometer (Cannon Instrument Co. 0C C108, State College, PA) was used to measure the viscosity of the cell solution at the beginning and at the end of each experiment.

5.2 Results and discussion

5.2.1 Viscosity of bacteria solution

The viscosity of the solution at the beginning and at the end of experiments conducted in polyimide and polypropylene units showed a small change during the experiment. The efflux time for the solution going through the bulb of the viscometer was 308 and 329 seconds at 30 °C, and 302 and 320 seconds at 35 °C. The average viscosity value was used in the Hagen-Poiseuille law to minimize the possible error by incorrect

Table 5.1: Summary of experimental procedures

Fiber units	No. of runs	Cell source	T (°C)	Flow rate (ml/min)	Sterilization	Note
HFM with chamber	4	Original suspended cells	37	35.7	no	New HFM unit
	1			11.4	no	New HFM unit
	1			25.4	no	Sterilized pre-used HFM unit
Silicon unit	1	Original suspended cells	30	35.7	no	
	1	Method 1		11.4	no	Stagnant for 6hrs
	1			11.4	no	stagnant for 12hrs
Polyimide unit	1	Method 2	30	25.4	no	
polypropylene unit	1	Original suspended cells	35	25.4, 11.4	yes	

Method 1 as described in section 5.1.4 with centrifuge; Method 2 as described in section 5.1.4 without centrifuge.

viscosity values. The density of bacteria solution was 0.999g/cm^3. The viscometer constant is 0.003026 mm^2/s^2 and the kinematic viscosity was calculated as the product of the efflux time and the viscometer constant. Thus the cell solution viscosity at 30 °C is:

Average efflux time = (308+329)/2 = 318. 5 s

$\nu_{average}$ = 0.003026 mm^2/s^2 × 318. 5 s = 0.964 mm^2/s

$\mu_{average} = \nu_{average} \times \rho$ =0.964 mm^2/s × 0.999 g/cm^3 = 0.00963 g/cm s

The correct viscosity can help to determine the baseline pressure drop vs. flow rate when the cell solution initially flowed through the fiber unit without any biofilm.

5.2.2 Cell growth in HFM unit

Experiments showed that in the five runs conducted with the HFM units, ΔP gradually increased during the initial four hours showing that the bacteria started to attach on the membrane. As shown in Figure 5.1, the increment of ΔP was different for each run, indicating different cell growth rates.

In the first run, ΔP started to increase dramatically after five hours. About twenty hours later, ΔP reached the highest point of 80 mmHg. The result shows that after reaching a certain biofilm thickness, cell detachment likely overcame the cell growth rate. Perhaps this was due to nutrient limitations or flow effects. In the second run, ΔP increased gradually. After 30 hours, fresh medium replaced cell suspension. At this point, ΔP continuously dropped to 19.8 mmHg twelve hours later. After replacing the fresh

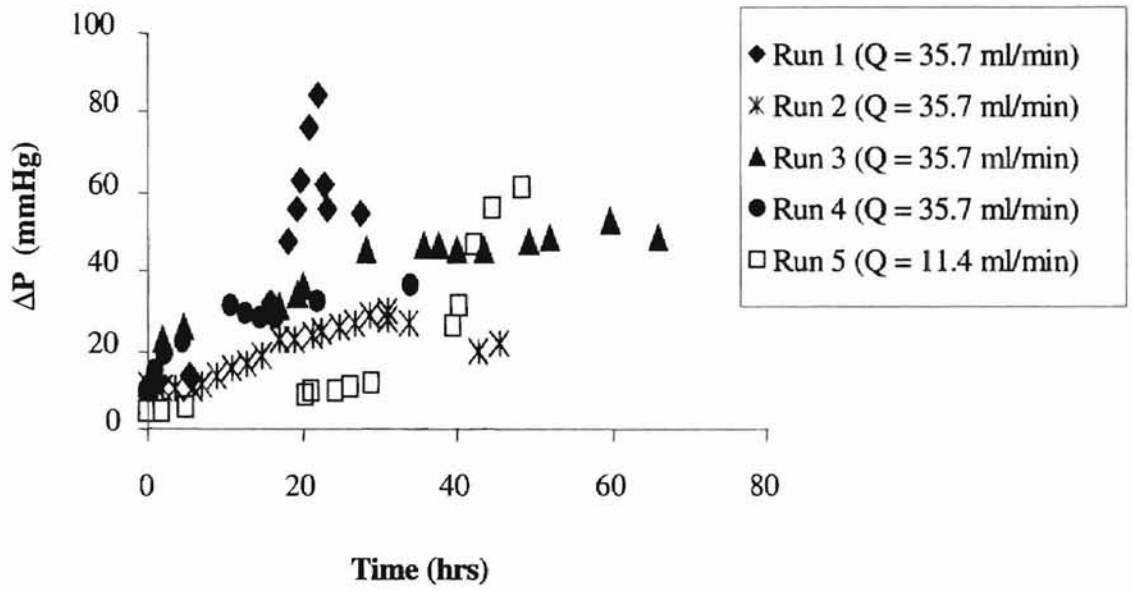

Figure 5.1 Cell growth in HFM unit. Cell suspensions flowed through the entire system. The increase of ΔP with time was measured. All five runs were conducted at approx37 °C, The flow rate was 35.7 ml/min in the first four runs and the fifth was at 11.4 ml/min.

medium with a cell suspension, ΔP increased back to 21.4 mmHg within three hours. In the third and fourth runs, biofilm growth was rapid because ΔP started to increase soon after each the experiment began. However, in the fifth run, the growth was slow for around 28 hours, afterwhich a dramatic increase in ΔP occurred. This may be the result of a low flow rate slowing down the initial attachment and growth, but afterwards cell growth increasing dramatically because less cell detachment occurred comparing to that at a higher flow rate.

For the fifth run, the fibers were cut into short pieces after the experiment and treated with cryofixation. However, no noticeable cells were found by SEM. One possible reason is that after the cryofixation treatment, the sample was frozen. When the sample was observed by SEM, the sample was melted and the cells were damaged by the charge. Moreover, SEM observations were conducted at 5KV, which provided a low resolution. Therefore, different fixation procedures were applied in later work.

In the sixth experiment, no obvious change of ΔP occurred. The initial reading of ΔP at time zero was 4.6 mmHg and remained at 4.9mmHg for 45 hours. This implied that no biofilm formed in the fibers. The difference between this run and the first five runs was that the HFM unit in the sixth experiment was sterilized following a previous use. Perhaps the sanitation procedure left some sterilant residue on the membrane which made it more difficult for cells to attach and grow on the membrane.

5.2.3 Cell Growth on platinum cured silicon unit

In the first experiment, the cell solution recirculated continuously in the system. The experiment showed no noticeable change of ΔP, which stayed at around 62-64

mmHg for 12 hours. Perhaps important nutrients in the medium had already been utilized. Therefore, the cell solution was centrifuged and pellets were resuspended in fresh medium. With a fresh suspension, there was a small increment in ΔP (see Figure 5.2) after the bacteria solution sat stagnant for six hours prior to circulation. Using the Hagen-Poiseuille law and the data of Figure 5.2, the change of ID of tubes, and hence the biofilm thickness can be predicted, as shown in Figure 5.3. Figures 5.4 and 5.5 show the lumen surface of the silicon unit, before and after the experiment, respectively.

Evidence shows that a thin biofilm grew on the silicon membrane, thus demonstrating pseudomonas aeruginosa could attach and grow on silicon membranes. However, it is difficult for the biofilm to grow thick. The average thickness of the biofilm was only about 5 μm (see Figure 5.6). However, the predicted biofilm thickness was 9.7 μm. Experimentally, the biofilm was so thin that the change of pressure drop was not dramatic. This small change of pressure drop is difficult to measure without some error, which may be the reason for the discrepancy. A more accurate pressure transducer would be required to assess thin biofilms.

Other parameters, such as flow rate, the ID of tubes, and cell solution viscosity also can affect the predictability of such a thin biofilm. A flow rate difference of 0.5ml/min could change the predicted biofilm thickness could be changed from 9 μm to 7.1 μm; if the measurement of viscosity increased 3%, the predicted thickness will drop to 7.5 μm; if the ID of tube decreased by 2%, the predicted biofilm thickness would decrease to only 4.8 μm. This demonstrats that the experimental set up including pressure transducer, the flowmeter and the accuracy of ID of tube were not sensitive enough to predict such a thin biofilm.

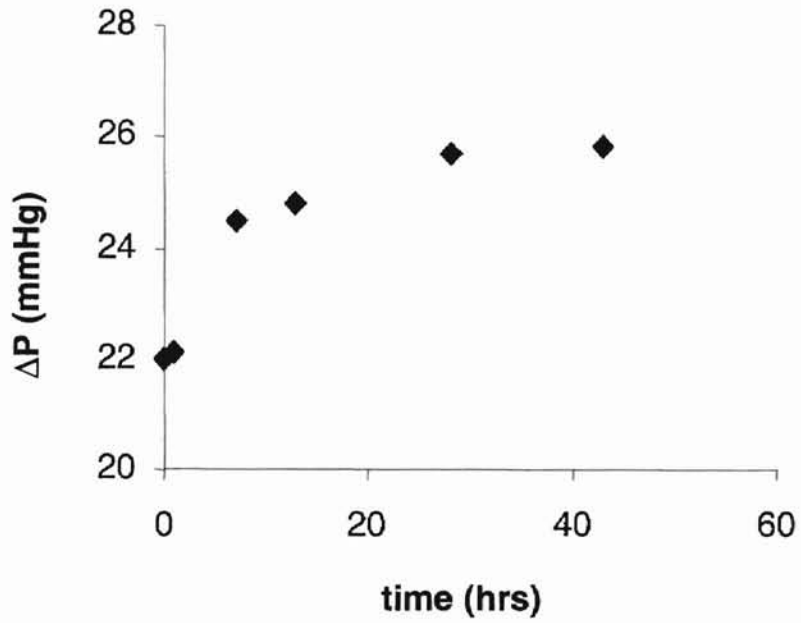

Figure 5.2 Pressure drop change across the platinum cured silicon unit. A Pseudomonas aeruginosa suspension remained stagnant at 30 °C. Afterwards, the suspension was circulated in the entire system at a flow rate of 11.4 ml/min.

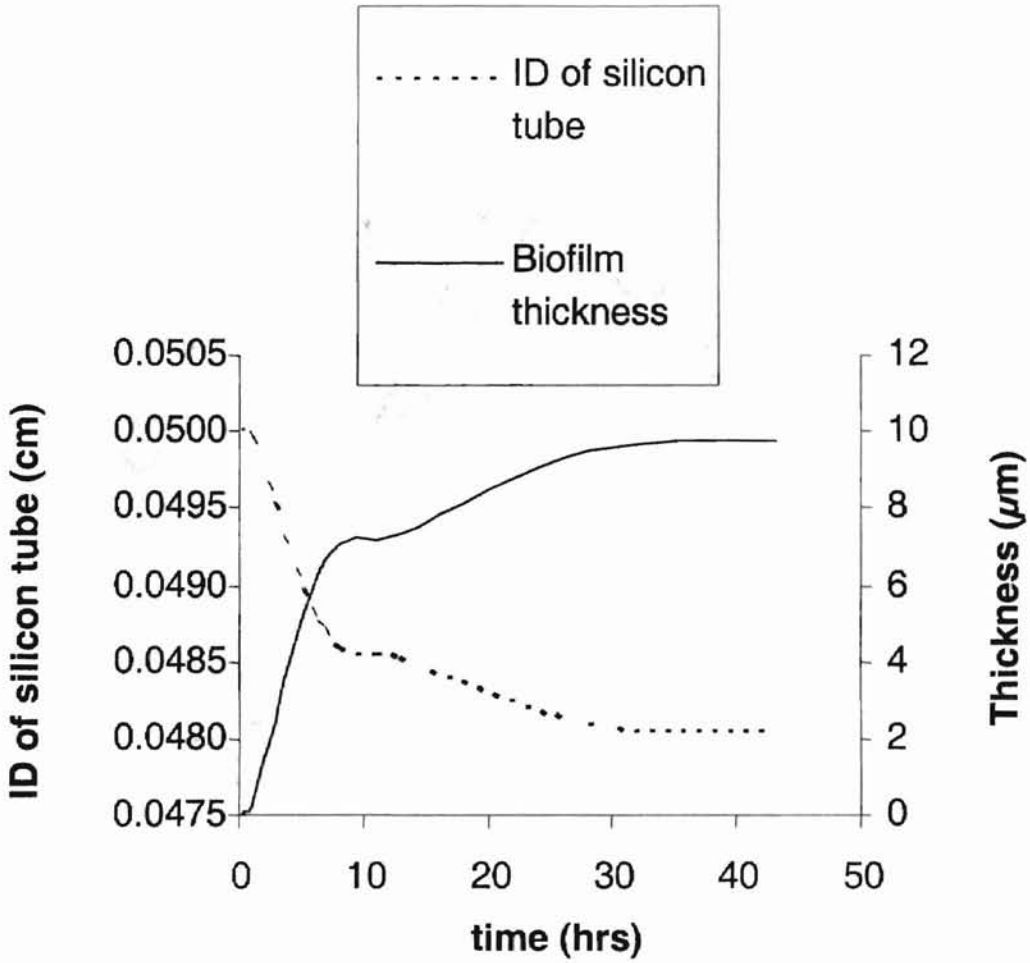

Figure 5.3 Prediction of biofilm thickness. The ID of the tube and hence the biofilm thickness in the silicon unit (second run) was estimated by applying the experimental ΔP to the Hagen-Poiseuille law. The culture conditions are summarized in Table 5.1.

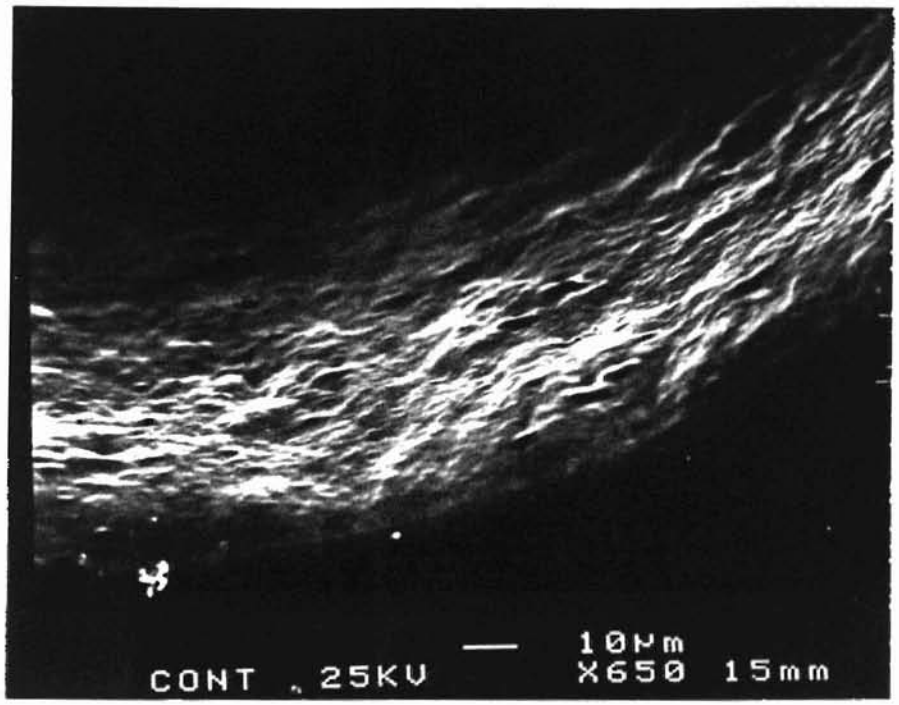

Figure 5.4 Silicon tubing without cells. Silicon tube without cells (before experiment) was cut into short pieces (1.5 cm) and the lumen surface of the silicon tube was examined as control by scanning electron microscope (SEM).

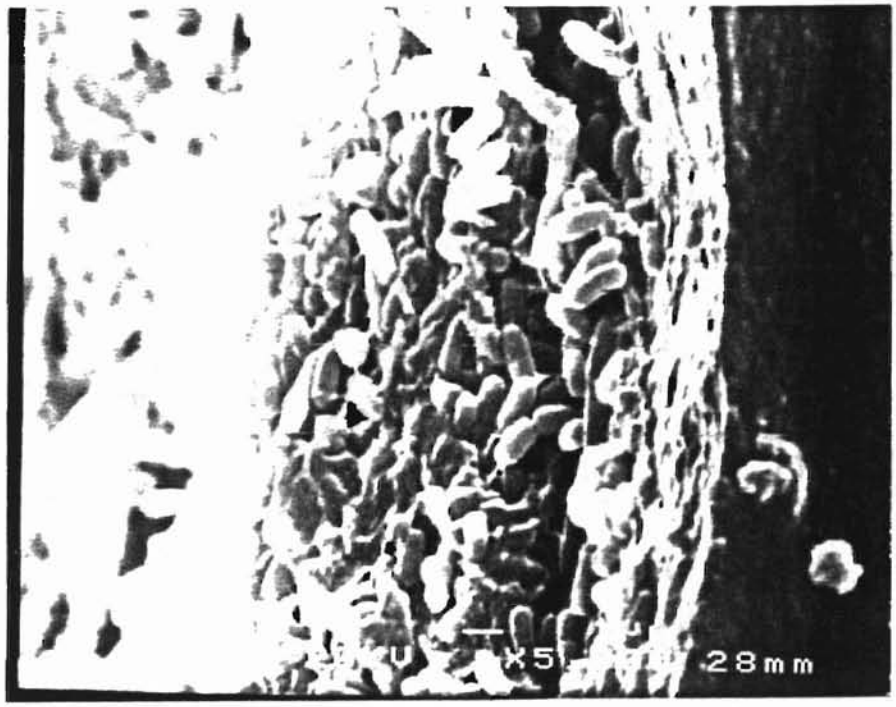

Figure 5.5 Cell growth in silicon tubing unit. After an experiment, the silicon unit was treated under glutaraldehyde fixation and cut to short pieces for the observation of cell growth inside the unit by SEM.

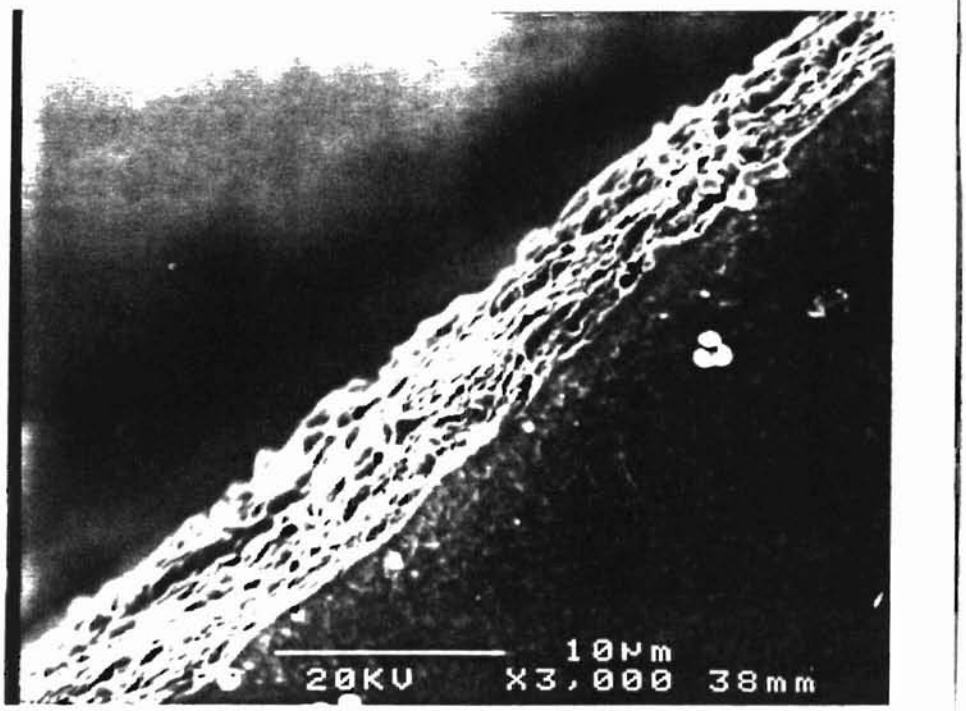

Figure 5.6 Biofilm thickness estimation from SEM in silicon unit. Biofilm thickness was estimated by averaging the biofilm thicknesses at different places (same run as in Figure 5.5).

In order to achieve a much thicker biofilm, the cell solution remained stagnant for 12 hours in the third run. Afterwards, the pump was turned on but there was very little change of ΔP as compared to a cell-free fiber unit. Correspondingly, the SEM showed that not many cells attached to the silicon membrane. The cells were sporadically found on the membrane. One possible reason for the lack of consistent attachment is the oxygen availability due to stagnant solution. Moreover, a platinum cured silicon tube has the tendency to resist cell attachment and growth on the surface. Therefore, two other polymer materials were tried: polyimide and polypropylene. Both materials are used for cell culture, especially polypropylene due to its high air permeability.

5.2.4 Cell growth on polyimide and polypropylene unit

For the polyimide unit, the ΔP increment was very small, changing from 8.85 to 10.75 mmHg. The SEM photos showed that very few cells attached and grew on the polyimide membrane as shown in Figure 5.7.

For the polypropylene tubing unit, unlike cell growth in the HFM unit with the same materials, there was no dramatic change in ΔP. ΔP increased from 11.8 to 15.9 mmHg at a flow rate at 25.4 ml/min following 23 hours. Afterwards, the flow rate was lowered to 11.4 ml/min to increase the chance of growing a thicker biofilm. ΔP changed from 8.3 to 16.0 mmHg after 74 hours. Comparing to the increment of ΔP for cell cultures in the HFM unit, this change was very small. The failure of biofilm formation by assessing ΔP may be the result of two factors: substrate concentration and membrane properties. When the bacteria solution was transferred to the fresh media, the concentration of the cells in the solution was very small. Since there were not many cells

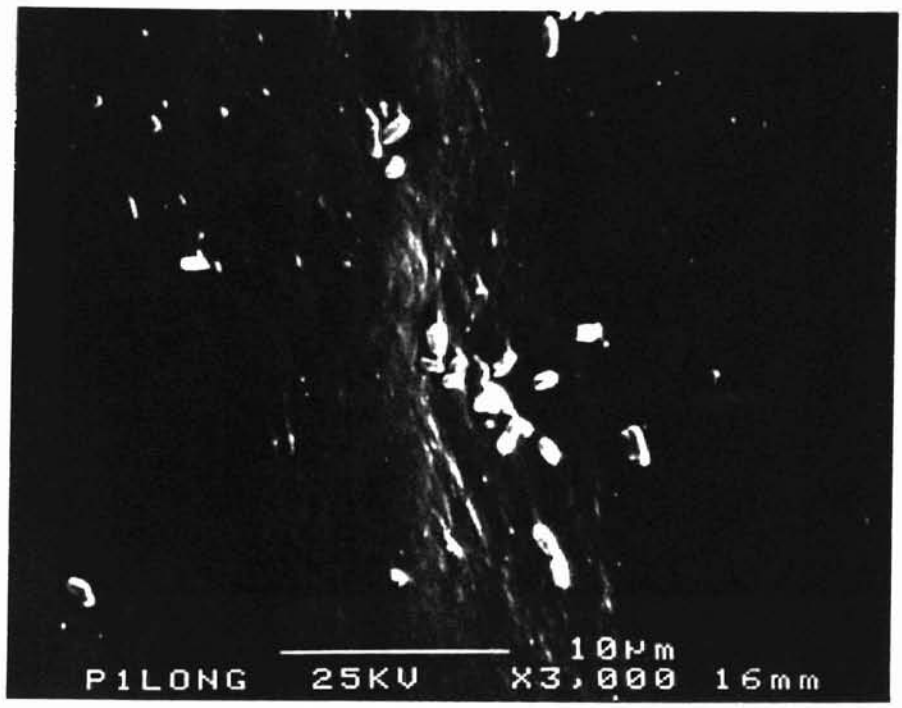

Figure 5.7 Cell growth in polyimide tubing unit. Cell solution circulated in the entire system at 30 °C at a flow rate of 25.8 ml/min. After the experiment, tubes were treated under gluteraldehyde fixation and cut into short pieces (1.5 cm).

available in the solution when it recirculated in the system, cell attachment and growth was limited by low loading concentration. Therefore, it was very difficult for cells to grow on the membrane. Another possibility is that polyimide has a very low permeability, and O_2 availability may have been a problem. Additives of polymer might also be a problem. Comparing growth in the HFM unit and the homemade polypropylene fiber unit, the difference in cell attachment may be caused by different additives that are added into the materials during the manufacturing process. The HFM unit and other polypropylene fiber system in literature are all manufactured for cell cultures. This difference might cause the different environment for cells to grow.

5.3 Conclusion

Experiments showed that cells could attach to surfaces in some of the fiber units although many units showed little attachment. With the proper fixation procedure, the SEM could be applied for studying biofilm thicknesses as a visual confirmation of theoretical prediction. However, the experimental set up in this research including pressure transducer, the flowmeter and the measurement of ID of tube were not sensitive enough to predict a very thin biofilm. As previously shown (see figure 4.3), only when the ΔP based on biofilm growth is at least three times as initial ΔP_i due to the fiber itself, the biofilm thickness is generally predictable. The alternative is to increase the sensitivity of the experimental set up.

Flow rate, oxygen availability, loading concentration, and properties of membrane may affect the potential biofilm growth. A low flow rate, high oxygen concentration and cell loading concentration may help cells to attach and grow on the membrane. The

properties of the membrane, such as high air permeability, non-toxicity of the membrane, and relatively rough surface can also help cell grow in the fiber unit.

Since it was difficult to form a biofilm in this research, the validation of the prediction of biofilm thickness by the Hagen-Poiseuille law could not be demonstrated. Moreover, experiments showed that the experimental set up is not sensitive enough for predicting a thin biofilm. However, from the conclusion of Chapter 4, monitoring ΔP across the fiber unit to predict the ID of tubes and the biofilm thickness may be useful if more sensitive validation equipment is utilized.

CHAPTER 6

CONCLUSION AND FUTURE WORK

Biofilms are involved in many areas, including food contamination, medical device related infections, treatment of wastewater and gas, and production of liquid fuel. The biofilm thickness is an essential parameter for studying biofilms. However, most methods for observation of biofilm growth and biofilm thickness are not *in-situ*, requiring cessation of experiments. This thesis objective was to predict the biofilm thickness in a hollow fiber membrane bioreactor (HFM) by monitoring ΔP across the fiber unit. The Hagen-Poiseuille law was utilized for the prediction. The research included three stages: validation of the Hagen-Poiseuille law in the HFM unit; modification of the HFM unit; and predictgion of biofilm formation and thickness.

Three specific aims were set to realize the objective. For the first stage of research, the validity of Hagen-Poiseuille law in HFM unit was examined. Water passed through the HFM unit and ΔP was measured at different flow rates. Experimental ΔP was compared with theoretical values calculated from the Hagen-Poiseuille law. Experiments showed the Hagen-Poiseuille law was not applicable for the original HFM units. The main reason appeared to be that water was not well distributed and not every fiber was used. This likely caused the discrepancy between experimental and theoretical values.

In the second stage, fiber systems were optimized for more accurate prediction of the fiber ID. The HFM units were modified to achieve better flow distribution and three other fiber units were made for convenient observation of the biofilm thickness. Experimental results showed that the Hagen-Poiseuille law is useful for prediction of ID

of fibers and is very accurate. For cell studies, consistent biofilm formation was difficult in either modified HFM units or homemade units. Thus it was difficult to validate the biofilm thickness using the Hagen-Poiseuille law. The experimental set up was not sensitive enough to predict a thin biofilm thickness. There was no increment of ΔP if no biofilm formed. However, biofilm thickness may still be predicted by the Hagen-Poiseuille law from the results in Chapter 4 if more sensitive equipment is used..

There are several suggestions for improving cell growth inside fiber systems and hence the predictability of biofilm thickness.

1. Experiments of cell cultures inside HFM units should be repeated to assess repeatability.
2. In order to provide enough nutrients available for cells during the experiment, fresh medium should be added and recirculated after initial attachment. Fresh nutrients will help the growth of cells.
3. HFM units can be ordered without plastic shells, therefore, cutting fibers to obtain a visual image of biofilm formation inside the fiber will be feasible..
4. More sensitive experimental equipment should be applied to improve the accuracy of the biofilm thickness prediction. Equipments includes flowmeter, pressure transducer, and visometer.
5. In order to determine a more reliable average biofilm thickness from SEM, statistical methods should be included.

In summary, this research was valuable for continuous study and biofilm growth and biofilm thickness in hollow fiber units. The study provided the possibility predicting

biofilm thickness by monitoring pressure drop across a hollow fiber unit. This method could be used to study biofilm growth *in situ* without interrupting the system. Thus, the method would be useful for controlling biofilm growth, obtaining optimal biofilm thickness, and hence optimizing hollow fiber bioreactors.

REFERENCES

1. Beyenal, H., Tanyolac, A., " The Effects of Biofilm Characteristics on the External Mass Transfer Coefficient in a Differential Fluidized Bed Biofilm Reactor". *Biochem. Eng. J.* **1**, 53-61.
2. Bird, B. R., Stewart, W. E., Lightfoot, E. N., "Transport Phenomena".
3. Bishop, P. L., Zhang, T. C., Fu, Y.-C., "Effects of biofilm Structure, Microbial Distributions and Mass Transport on Biodegradation Processes". *Wat. Sci. Tech.* **31** (1), 143-152.
4. Blanch, H. W., Clark, D. S., "Biochemical Engineering".
5. Bober, W., Kenyon, R. A., "Fluid Mechanics".
6. Brindle, K. Stephenson, T., Semmens, M. J., "Nitrification and Oxygen Utilization in a Membrane Aeration Bioreactor". *J. Mem. Sci.* **144**, 197-209.
7. Broch-Due, A., Andersen , R., Opheim, B., "Treatment of Integrated Newsprint Mill Wastewater in Moving Bed Biofilm Reactors". *Water. Sci. Tech.* **35** (2-3), 173-180.
8. Brower J. B., Barford, C. C., Hao, O. J., "Biological Fixed-film Systems". *Water Environ. Res.* **68**, 469-479.
9. Bryers, James D., Drummond, F., "Local Macromolecule Diffusion Coefficients in Structurally Non-Uniform Bacterial Biofilms Using Fluorescence Recovery After Photobleaching (FRAP)". *Biotechnology and Bioengineering* **60** (4), 462-473.
10. Cao, Y. S., Alaerts, G. J., "Influence of Reactor Type and Shear Stress on Aerobic Biofilm Morphology, Population and Kinetics". *Wat. Res.* **29** (1), 107-118.

11. Capiaumont, J., Legrand, C., Carbonell, D., Dosset, B., Bellville, F., Nabet, P., "Methods for Reducing the Ammonia in Hybridoma Cell Cultures". *J. Biotech.* **39**, 49-58.

12. Casey, E., Glennon, B., Hamer, G., "Oxygen Mass Transfer Characteristics in a Membrane –Aerated Biofilm Reactor". *Biotech. Bioeng.* **62**, 193-192.

13. Cheng, Sheng-Shung, Chen, Wen-Chin, Hwang, Hui-Hsiang, "Biofilm Formation: The Effects of Hydrodynamic and Substrate Feeding Patterns in Three Phase Draft-Tube Fluidized Bed for Nitrificcation Process". *Wat. Sci. Tech.***36** (12), 83-90.

14. Corsi, R. L., Seed, L., "Biofiltration of BTEX: Media, Substrate and Loading Effects"

15. Costerton, J. W., Stewart, P. S., Greenberg E. P., "Bacterial Biofilms: A Common Cause of Persistent Infections". *Science,* **284**, 1318-1322.

16. Costerton, J.W., "Introduction to Biofilm". *Intl. J. Antimicrob. Agents* **11**, 217-221.

17. Cunnlngham, Alfred S., William, G. Characklls, Felsa Abedeen, Crawford, David, "Influence of Biofilm Accumulation on Porous Media Hydrodynamics". *Eviron. Sci. Technol.* **25**, 1305-1311

18. Das, A., Abou-Nemeh, I., Chandra, S., Sirkar, K. K., "Membrane-moderated Stripping Process for Removing VOC's from Water in a Composite Hollow Fiber Module". *J. Mem. Sci.* **148**, 257-271.

19. Davis, J. M., Hanak, J. A. J., "Hollow –Fiber Cell Culture". *Meth. Molecular Bio.* **75**, 77-89.

20. Dijk, L. van, Roncken, G. C. G., "Membrane Bioreactors for Wastewater Treatment : the State of the Art and New Developments". *Wat. Sci. Tech.* **35** (10), 35-41.

21. Dowd, J. E., Weber, I., R, Beatriz., Piret, J. M., Ezra Kwok, K., "Predictive Control of Hollow-Fiber Bioreactors for the Production of Monoclonal Antibodies" . *Biotechnol. Bioeng.* **63**, 484-492.

22. Drioli, E., Giorno, L., "Biocatalytic Memebrane Reactors: Application in Biotechnology and the Pharmaceutical Industry".

23. Dront, M., Sam, F. M., Adler, N., Peringer, P., "Biomass Growth Monitoring Using Pressure Drop in a Cocurrent Biofilter". *Biotechnol. Bioeng.* **60** (1), 97-104.

24. Drury, W. J., Characklis, W. G., Stewart, P. S., "Interactions of 1μm Latex Particles With Pseudomonas Aeruginosa Biofilms". *Wat. Res.* **27** (7), 1119-1126.

25. Edgehill, R. U., " Degradation of Pentachlorophenol (PCP) by Arthrobacter Strain Atdie. CC 33790 in Biofilm Culture". *Wat. Sci. Tech.* **30** (2), 357-363.

26. Ergas, S. J., McGrath, M. S., "Membrane Bioreactor for Control of Volatile Organic Compound Emissions". J. Environ. Eng. June/1997, 593-598.

27. Ergas, S. j., Shumway, L., Fitch, M. W., Neemann, J. J., "Membrane Process for Biological Treatment of Contaminated Gas Streams". *Biotechnol. Bioeng.* **63**, 431-441.

28. Fava, F., Gioia, D. D., Marchetti, L., "Dichlorobiphenyl Degradation by an Uncharacterized Pseudomonas Species, Strain CPE1, in a Fixed Film Bioreactor". *Intl. Biodeteerioration & Biodegradation* (1996), 53-59.

29. Ferreira Bruno S., Fernandes, Helena L., Reis, Alberto, Mateus, Marilia, "Microporous Hollow Fiber ofr Carbon Dioxide Absorption: Mass Transfer Model Fitting and the Supplying of Carbon Dioxide to Microalgal Cultures". *J. Chem. Technol.* **71**, 61-70.

30. Freitas dos Santos, L. M., Hommerich, U., Livingston, A. G., "Dichloroethane Removal from Gas Streams by an Extractive Membrane Bioreactor". *Biotechnol. Prog.* **11**, 194-201.

31. Freitas dos Santos, L. M., Livingston, A. G., "Membrane –Attached Biofilms for VOC Wastewater Treatment. II: Effect of Biofilm Thickness on Performance". *Biotechnol. Bioeng.* **47**, 90-95.

32. Ganesh, Kumar C. and Anand, S. K., "Significance of microbial biofilms in food industry: a review".

33. Gramer, A. J., Poeschl, D. M., "Screening toll for Hollw Fiber Bireactor Process Development". *Biotechnol. Prog.* **14**, 203-208.

34. Grethlein, A. J., Woerden, R. M., Jain, M. K., Datta, R., "Continuous Production of Mixed Alcohols and Acids from Carbon Monoxide". *Applied Biochem. Biotech.* **24/25**, 875-885.

35. Handa-Corrigan, A., Nikolay, S., Jeffery, Heffernan, D., B., Young, A., "Controlling and Predicting Monoclonal Antibody Production in Hollow Fiber Bioreactors". *Enzyme Micob. Technol.* **14**, 58-63.

36. Jauregui, H. O., Naik, S., Santangini, H., Pan, J., Trenkler, D., Mullon, C., "Primary Cultures of Rat Hepatocytes in Hollow Fiber Chambers". *In Vitro Cell. Dev. Biol.* **30A**, 23-29

37. Jayaraman, V. K., " The Solution of Hollow Fiber Bioreactor Design Equations". *Biotechnol. Prog.* **8**, 462-464.

38. Kamo, Uchida, M., Hirai, T., Yosida, H., Kamada, K., Takemura, T., "A New Multilayered Composite hollow Fiber Membrane for Artifical Lung". *Artificial Organs* **14**, 369-472.

39. Klasson, K. T., Ackerson, M. D., Clausen, E. C., Gaddy, J., "Bioconversion of Synthesis Gas into Liquid or Gaseous Fuels". *Enzyme Microb. Technol.* **14**, 602-608.

40. Kuroda, M., Watanabe, T., Umedu, Y., "Simultaneous Oxidation and Reduction Treatments of Polluted Water by a Bio-electro Reactor". *Wat. Sci. Tech.* **34** (9)101-108.

41. Langwaldt, J.H., Puhakka, J. A., "On-site Biological Remediation of Contaminated Groundwater: a Review". *Eviron. Pollution* **107**, 187-197.

42. Lazarova, V., Manem, J., "Advances in Biofilm Aerobic Reactors Ensuring Effective Biofilm Activity Control". *Wat. Sci. Tech.* **29** (10-11), 319-327.

43. Lazarova, V., Manem, J., "Biofilm Characterization and Activity Analysis in Water and Wastewater Treatment". *Wat. Res.* **29** (10), 2227-2245.

44. Lowrey, David, Murphy, Susan, Goffe, Randal A., "A comparison of Monoclonal Antibody Productivity in Different Hollow Fiber Bioreactors". *J. of Biotech.* **36**, 35-38

45. Miller, A. O. A., Menozzi, F. D., Dubois, D., "Microbeads and Anchorage-Dependent Eukaryotic Cells: The Beginning of a New Era in Biotechnology". *Adv. Biochem. Eng. Biotech.* **39**,73-96.

46. Molinar, F., Aragozzini, F., Cabral, J. M. S., Prazeres, D. M. F., "Continuous Production of isovaleraldehyde through Extractive Bioconversion in a Hollow Fiber Membrane bioreactor". *Enzyme Microb. Technol.* **20**, 604-611.

47. Molinari, R., Torres, J. L., Michaels, A. S., Kilpatrick, P. K., Carbonell, R. G.,"Simultaneous Ultrafiltration and Affinity Sorptive Separation of Proteins in a Hollow Fiber Membrane Module". *Biotehnol. Bioeng.* **36**, 572-580.

48. Nicolella, C., Pavasant, P., Livingston, A. G., "Substrate Counterdiffusion and Reaction in Membrane-attached Biofilms: Mathematical Analysis of rate Limiting Mechanisms". *Chem. Eng. Sci.* **52**, 1385-1398.

49. Nordon, R. E., Schindhelm, K., " Design of Hollow Fiber Modules for Uniform Shear Elution Affinity Cell Separation". *Artificial Organ* **21** (2), 107-115.

50. Pankhania, M., Brindle, K., Stephenson, T., "Membrane Aeration Bioreactors for Wastewater Treament: Completely Mixed and Plug flow Operation". *Chem. Eng. J.* **73**, 131-136.

51. Parvatiyar, M. G., Govind, R., Bishop, D. F., " Biodegradation of Toluene in a Membrane Biofilter". *J. Mem. Sci.* **119**, 17-24.

52. Peys, K., Diels, L., Leysen, R., Vandecasteele, C., "Development of A Membrane Biofilm Reactor for the Degradation of Chlorinated Aromatics". *Wat. Sci. Tech.* **36** (1), 205-214.

53. Phillips, J. R., Clausen, E. C., Gaddy, J. L., "synthesis Gas as Substrate for the Biological Production of Fuels and Chemicals". *App. Biochem. Biotech.* **45/46**, 145-157.

54. Phillips, J. R., Klasson, K. T., Clausen, E. C., Gaddy, J. L., "Biological Production of Ethanol from Coal Synthesis Gas". *Appl. Biochem. Biotech.* **39/40** (1993), 559-571.

55. Prokop, A., Rosenberg, M. Z., "Bioreactor for Mammalian Cell Culture". *Adv. Biochem. Eng. Biotech.* **39**, 29-72.

56. Pujol, R., Canler J. P., Iwema, A., "Biological Aerated Filters: An attractive and Alternative Biological Process". *Wat. Sci. Tech.* **26** (3-4), 693-702.

57. Reij, M. W., Hamann, E. K., Harmans, S., "Biofiltration of Air Containing Low Concentrations of Propene Using a Membrane Bioreactor". *Biotechnol. Prog.* **13**, 380-386.

58. Reij, M. W., Hartmans, S., "Propene Removal from synthetic Waste Gas Using a Hollow-Fiber Membrane Bioreactor". *Appl. Microbiol. Biotechnol.* **45**, 730-736.

59. Rejj, M. W. Keurentjes, J. T. F. Harmans, S., "Membrane Bioreactors for Waste Gas Treatment". *J. Biotech.* **59**, 155-167.

60. Revah, S., Lobo, R., Viveros-Garcia, T., "An analysis of a Trickle-bed Bioreactor: Carbon Disulfide Removl"

61. Sajc, L., Grubisic, D., Vunjak-Novakovic, G., "Bioreactors for Plant Engineering: an Outlook for Further Research". *Biochem. Eng. J.* **4**, 89-99.

62. Sassi, G., Ruggeri, B., Bosco, F., Specchia, V., "Relaxation Time Analysis of a Rotating Biological Contactor". *Chem. Eng. Sci.* **51** (11), 2853-2858.

63. Schugerl, K., Oels, U., Lucke, J., "Bubble Column Bioreactors". *Adv. Biochem. Eng. Biotech.* **7**, 1-84.

64. Schweikart, F., Jones, R., Jaton, J. C., Hughes, G. J., "Rapid Structural Characterisation of a Murine Monoclonal IgA Chain: heterogeneity in the Oligosaccharide Structues at a Specific Site in Samples Produced in Different Bioreactor Systems". *J. Biotech.* **69**, 191-201.

65. Seker, S., Beyenal, H., Tanyolac, A., "The Effects of Biofilm Thickness on biofilm Density and Substrate Consumption Rate in a Differential Fluidized Bed Biofilm Reactor". *J. Biotech.* **41**, 39-47.

66. Sreve, G. S., Olsen, R. H., Vogel, T. M., "Development of Pure Culture Biofilms of P. putida on Solid Supports". Biotechnol. Bioeng. 37, 512-518.

67. Stewart, P. S., "A Model of Biofilm Detachment". *Biotechnol. Bioeng.* **41**, 111-117.

68. Stoll, T. S., Ruffieux, P.-A., von Stockar, U., Marison, I. W., "Development of an On-line Control System for the Cultivation of Animal Cells in a Hollow Fiber Reactor using flow injection analysis and a visual programming language". *J. Biotech.* **51**, 37-48.

69. Tanyolac, A., Beyenal, H., "Effective Factor for a Hollow-Fiber Biofilm Reactor at Maximum Substrate Consumption". *chem. Eng. J.* **62**, 149-154.

70. Tanyolac, A., Beyenal, H., "Prediction of substrate consumption rate, average Biofilm Densisty and Active Thickness for a Thin Spherical Biofilm at pseudo-steady State". *Biochem. Eng. J.* **2** (1998), 207-216.

71. Van Loosdrecht, M.C. M., Eikelboom, D., Gjaltema, A., Mulder, A., Jijhuis, L., Heijnen, J. J., "Biofilm Structure". *Wat. Sci. Tech.* **32** (8) 35-43.

72. Villaverde, S., Mirpuri, R., Lewandowski, Z., Jones, W. L., "Study of Toluene Degradation Kinetics in a Flat Plate Vapor Phase Bioreactor Using Oxygen Microsensors".

73. Wanner, O., "New Experimental Findings and Biofilm Modelling Concepts". *Wat. Sci. Tech.* **32** (8), 133-140.

74. Yamaguchi, T.. Ishida, M., Suzuki, T., "Biodegradation of Hydrocarbons by Prototheca zopfii in Rotating Biological Contactors". *Process Biochem.* , 403-409.

VITA

Chun Li

Candidate for the degree of

Master of Science

Thesis: PREDICTION OF BIOFILM THICKNESS IN HOLLOW FIBER BIOREACTORS

Major field: Chemical Engineering

Biographical:

Personal Data: Born in Chengdu, P. R. China, on October 14, 1974.

Education: Graduated from Yan Shiko High school, Chengdu, Sichuan, P. R. China in July 1993

Received Bachelor of Science degree in Polymer Materials & Science in Sichuan Union University, Chengdu, Sichuan, P. R. China in July 1997

Completed the requirements for the Master of Science degree with a major in Chemical Engineering at Oklahoma State University in July, 2000.

Experiences: Employed as a material engineer in Technical Center at Chengdu Telecommunication Cable Company, China

Employed by Oklahoma State university, Department of Chemical Engineering as Graduate Research assistant, 1998-1999

Employed by Oklahoma State university, Department of Chemistry as Graduate Teaching assistant, 1999-2000.